



**Ana Catarina
Monteiro Magalhães**

**Habitáculo para peixe zebra para imagens PET:
controlo das condições ambientais e de sinais vitais**

**Zebrafish enclosure for PET imaging: control of the
environmental conditions and vital signs**



**Ana Catarina
Monteiro Magalhães**

**Habitáculo para peixe zebra para imagens PET:
controlo das condições ambientais e de sinais vitais**

**Zebrafish enclosure for PET imaging: control of the
environmental conditions and vital signs**

Dissertação apresentada à Universidade de Aveiro para cumprimento dos requisitos necessários à obtenção do grau de Mestre em Engenharia Biomédica, realizada sob a orientação científica da Professora Doutora Ana Luísa Silva, Professora Auxiliar do Departamento de Física da Universidade de Aveiro e do Doutor Pedro Manuel Mendes Correia, do Departamento de Física da Universidade de Aveiro

This project was supported by: A) project iPET CENTRO-01-0247-FEDER-039880, co-financed by the EU through FEDER; B) PTDC/EMD-EMD/21402020; and C) grant to Ana Catarina Monteiro Magalhães through the FCT, Portugal.

o júri / the jury

presidente / president

Professor Doutor Augusto Marques Ferreira da Silva

Professor Associado da Universidade de Aveiro

vogais / examiners committee

Doutora Susana Manuela Martinho dos Santos Baía Brás

Investigadora no Instituto de Engenharia Electrónica e Telemática de Aveiro (IEETA) da Universidade de Aveiro

Professora Doutora Ana Luísa Monteiro Silva

Professora Auxiliar do Departamento de Física da Universidade de Aveiro (orientadora)

**agradecimentos /
acknowledgements**

Em primeiro lugar gostaria de agradecer aos meus orientadores, à Professora Doutora Ana Luísa Silva e ao Doutor Pedro Correia, por todo o acompanhamento e preciosa ajuda ao longo deste percurso. Obrigada por toda a simpatia com que me acolheram e por todas as partilhas de conhecimento e de experiências.

Gostaria de agradecer aos membros do grupo DRIM, pelas trocas de conhecimento, pelo bom ambiente de trabalho e entreaajuda. Em especial gostaria de agradecer à Regina pelo companheirismo e entreaajuda nas horas de trabalho e pelos bons momentos. Ao Professor Doutor João Veloso, pela partilha de valiosos conhecimentos e ideias.

Também gostaria de agradecer à Doutora Inês Domingues, responsável pelos peixes zebra do biotério do Departamento de Biologia da Universidade de Aveiro, pela paciência e pela sua pronta disponibilidade em cooperar.

Agradeço também aos meus colegas do curso por estes incríveis 5 anos. Um obrigado especial à Carolina, à Cátia, à Simone, à Andreia e à Ana pelo carinho e amizade com que sempre me presentearam, tanto em momentos de trabalho como de convívio.

Por fim, um agradecimento especial a toda a minha família, principalmente aos meus pais, à minha irmã, e ao meu namorado, por todo o apoio, amor, carinho e paciência ao longo deste percurso.

A todos, o meu muito obrigado!

Palavras-chave

Habitáculo, condições ambientais, batimento cardíaco, imagem médica, estabilidade fisiológica, peixe zebra

Resumo

O peixe zebra tem vindo a demonstrar ser um excelente modelo animal para a investigação em diversas áreas da biomedicina, uma vez que apresenta características únicas, como o baixo custo, simplicidade de manutenção, curto ciclo de vida, genoma sequenciado, que facilita a sua manipulação genética e alguns mecanismos fisiológicos semelhantes aos do ser humano. Em investigação pré-clínica, muitas vezes, é necessário avaliar determinados processos metabólicos que ocorrem no interior dos modelos animais em estudo. Para isso, recorre-se usualmente a técnicas de imagem molecular e funcional, como por exemplo a Tomografia por Emissão de Positrões (PET do inglês *Positron Emission Tomography*). Contudo, este tipo de técnica médica exige que o animal esteja vivo, o que, em certa medida, acarreta uma dificuldade acrescida relativamente aos sistemas de imagem morfológica. No presente trabalho pretende-se desenvolver um habitáculo para peixes zebra que permita realizar a aquisição de imagens PET *in vivo*, enquanto se monitoriza, em tempo real, o bem-estar do animal, através da análise do batimento cardíaco do mesmo.

Assim, o habitáculo do peixe zebra foi pensado, desenhado e contruído em conjunto com o sistema de monitorização dos sinais vitais (LED infra vermelho e fotodíodo) e da temperatura da água (termístor). O sistema desenvolvido foi testado com peixes zebra em condições controladas e simultaneamente foram adquiridos vídeos dos peixes zebra, onde visualmente é possível quantificar o batimento do coração e dos opérculos por métodos de visão computacional. A gama de valores obtidos por ambos os métodos para o batimento cardíaco do peixe zebra foi de 80 - 130 bpm, conforme esperado. Além disso, também se verificou que o movimento do opérculo dificulta a medição do batimento cardíaco, contudo o seu efeito pode ser atenuado. Assim, o sistema desenvolvido tem a particularidade de monitorizar tanto a temperatura da água como os sinais vitais do peixe zebra, garantindo a sua estabilidade fisiológica durante os exames de imagem médica.

Keywords

Enclosure, environmental conditions, heart rate, medical imaging, physiological stability, zebrafish

Abstract

The zebrafish has emerged as an excellent animal model for studies in research in several areas of biomedicine because it has unique characteristics, such as low cost and simplicity of maintenance, short life cycle, sequenced genome, which facilitates its genetic manipulation, and some physiological mechanisms similar to human beings. In preclinical research, it is often necessary to evaluate certain metabolic processes that occur within the animal models under study. For this, molecular and functional imaging techniques are usually used, such as Positron Emission Tomography (PET) . However, this type of medical technique requires the animal to be alive, which, to a certain extent, entails an additional difficulty of morphological imaging systems. In the present work, a zebrafish enclosure was developed to allow the acquisition of PET images *in vivo*, while monitoring, in real time, the animal's well-being through the analysis of their heart rate.

Thus, the zebrafish enclosure was designed, developed and built together with vital signs (infrared LED and photodiode) and water temperature (thermistor) monitoring system. Furthermore, the developed system was tested with zebrafish under controlled conditions, and videos of the zebrafish were simultaneously acquired once it is visually possible to quantify the heart-beat and operculum using computer vision methods. The range of values obtained by both methods for zebrafish heart rate was 80 - 130 bpm, as expected. Moreover, it has also been found that the movement of the operculum makes it challenging to measure the heart rate, but its effect can be attenuated. Thus, the developed system has the particularity of monitoring the water temperature and the zebra fish's vital signs, ensuring physiological stability during medical imaging exams.

Contents

List of Acronyms	iii
List of Figures	iv
List of Tables	1
1 Introduction	2
2 Zebrafish as an animal model	4
2.1 Influence of the environmental conditions	6
2.2 Emerging fields of research	8
2.3 Anaesthesia	10
3 Imaging techniques used on zebrafish	12
3.1 Positron Emission Tomography	12
3.1.1 Physical principles	12
3.1.2 Studies with zebrafish models	15
3.2 Other imaging techniques conducted on zebrafish	18
3.2.1 MRI	18
3.2.2 Ultrasonography	19
3.2.3 Electrocardiography	19
4 Ethics and protocols for zebrafish preparation	21
5 Zebrafish Enclosure	23
5.1 Design proposal	23
5.2 Monitoring system	25
5.2.1 Heartbeat conditioning circuit	27

5.2.2	Water temperature conditioning circuit	28
5.2.3	Firmware	29
5.2.4	Software and Graphical User Interface	29
5.2.5	Computer vision for heart rate detection	33
6	Evaluation and validation of the acquisition environment	34
6.1	Dissolved oxygen and pH measurements	34
6.2	Water temperature measurements	36
6.3	Validation of the vital signs monitoring system	36
7	Zebrafish vital signs measurements	38
8	Conclusion	48
8.1	Future Work	49
	Bibliography	50

List of Acronyms

ADC Analog-to-Digital Converter.

BBB Blood-Brain-Barrier.

CT Computed Tomography.

DC Direct Current.

DESI-MS Desorption Electrospray Ionisation - Mass Spectrometry.

FFT Fast Fourier Transform.

GUI Graphical User Interface.

IR LED infrared light-emitting diode.

ISR Interrupt Service Routine.

LOR Line of Response.

MRI Magnetic Resonance Imaging.

MS222 tricaine methanesulfonate.

NTC Negative Temperature Coefficient.

OPAMP Operational Amplifier.

PCB Printed Circuit Board.

PET Positron Emission Tomography.

PMMA *Poly(methyl methacrylate)*.

ROI Region of Interest.

List of Figures

2.1	a) Anatomy of adult zebrafish. Adapted from [6]. b) Anatomy of the zebrafish heart. Adapted from [7].	4
3.1	Diagram of the positron emission during the decay process of a radionuclide and the annihilation process. Adapted from [31].	13
3.2	Process of the PET image acquisition. Adapted from [35].	14
3.3	Representative scheme of the signals acquisition from an annihilation event. Adapted from [33].	14
3.4	Physical phenomena that can occur from annihilation to detection (during the acquisition of PET images). The black dots indicate the position of the annihilation of the positron with the electron. Adapted from [37]	15
3.5	a) PET image of zebrafish 20 minutes after removing the fish from the tank with the ^{18}F -FDG . Adapted from [38]. b) PET /CT imaging of ^{18}F -FDG (20 MBq injected) 30 min after the intraperitoneal injection. Adapted from [23].	16
3.6	PET images of [^{18}F] FTHA tracer. Adapted from [39]	17
3.7	Zebrafish MRI flow cell system. Adapted from [1].	18
3.8	Block diagram of a high-resolution ultrasonic system for studying the cardiovascular system of an adult zebrafish. Adapted from [25].	19
3.9	a) Immobilisation and positioning of electrodes for ECG acquisition in zebrafish. b) ECG obtained. Adapted from [7].	20
4.1	Anaesthesia protocol followed in the present dissertation.	22
5.1	a) Design of the immobilisation block of the zebrafish's bed. b) Design of the cylinder that wraps around the immobilisation block, closing the container. .	24
5.2	Design of two different bed prototypes. a) "V" shaped bed, with less volume and easier to place and remove the piece. b) "V" shaped bed, with more volume and more difficulty to place and remove the piece.	24
5.3	Upgrade of the design of the zebrafish bed. a) The bed shape changed to a trapeze. b) The sensor holes in the bed were expanded.	25

5.4	Zebrafish in the bed with a sponge to improve immobilisation.	25
5.5	Sensor arrangement relative to the zebrafish (front view).	26
5.6	Block diagram of the heartbeat and water temperature measurement and display.	27
5.7	Signal conditioning circuit a) Heartbeat conditioning circuit. b) Thermistor conditioning circuit.	28
5.8	Image of the final version of the sensors positioning in the bed and waterproofed.	28
5.9	Block diagram of the Python script structure.	30
5.10	Detailed description of the role of each process and thread.	31
5.11	Graphical interface developed, during the signal acquisition.	32
5.12	Interface of the computer vision software.	33
6.1	Setup to measure the dissolved oxygen and pH of the water a) with a magnetic stirrer, and b) without a magnetic stirrer.	35
6.2	Variation of the a) concentration of dissolved oxygen and b) the pH over time with zebrafish and without (control).	35
6.3	Water temperature evolution during a zebrafish trial.	36
6.4	Graphics that compare the heart rate values obtained by the developed system's sensors and a commercial heart rate meter in two different volunteers.	37
7.1	Setup used in trial 1.	39
7.2	Block diagram of the analysis applied to the acquired signals, both by the sensors and the camera.	40
7.3	Signal acquired from zebrafish 1.1.	41
7.4	Signal acquired from zebrafish 1.2. a) At the beginning, signal with slow opercular movement (peaks with higher intensity) and with heartbeat pulses between the operculum peaks. b) FFT of the filtered signal represented in a) and respective Gaussian sum curve adjusted.	41
7.5	Signals acquired by the sensors (blue) and by the camera (orange) towards the end with only heart movement from a) zebrafish 1.2 and b) zebrafish 1.4.	42
7.6	Signal acquired from zebrafish 1.5, correspondent to the opercular movement and respective zoom of the signal.	42
7.7	Box plot representing the dispersion of the time difference between the same sensors and video peaks of the zebrafish 1.2 and 1.4 signals.	43
7.8	Signal acquired from zebrafish 2.1 and respective zoom of the signal.	45
7.9	Signals acquired by the sensors (blue) and by the camera (orange) from zebrafish 2.2.	45
7.10	Signals acquired from zebrafish 2.4. a) General view of the signal. b) Particular region of the signal with only heart movement.	46

7.11	Box plot representing the dispersion of the time difference between the same sensors and video peaks of the zebrafish 2.2 and 2.4 signals.	47
------	--	----

List of Tables

2.1	Optimum range of environmental water parameters for zebrafish.	6
2.2	Main advantages of the zebrafish models in different areas of research.	8
2.3	Stages of anaesthesia and the consequent effect in several behavioural criteria. (Adapted from [27]).	11
2.4	Influence of different anaesthesia and different concentrations on the zebrafish heart rate.	11
7.1	Identification of the zebrafish used in trial 1.	39
7.2	Zebrafish heart and operculum rates calculated using three different approaches applying the algorithm <i>find_peaks</i> in the sensors and the video signals, and the mean value of a Gaussian curve adjusted to the FFT of the signal obtained by the sensors.	43
7.3	Identification of the zebrafish used in the trial 2.	44
7.4	Zebrafish heart and operculum rates calculated using two different approaches applying the algorithm <i>find_peaks</i> in the sensors signal, and applying the algorithm <i>find_peaks</i> in the video signal.	46

Chapter 1

Introduction

Given the great challenge of researching in humans, including ethical issues, most experimental studies are conducted in animal models, traditionally mammals like rodents. The reason for this is mainly due to the homology of the mammalian genome, anatomy, cellular biology, and physiology [1]. However, these models have also some disadvantages, such as the high maintenance cost and complex genomes [2]. On the other hand, non-mammalian vertebrates, particularly fishes, have genetic, endocrine, and physiological features, brain mechanisms and essential gut functions similar to humans. These similarities allow using fishes as models of human diseases.

Additionally, fishes like zebrafish have short life cycles and a low maintenance cost compared to mammalian models, facilitating surgeries and genetic manipulation [2]. These aspects make large-scale studies far timelier and more economical than it is possible with other vertebrate models. Furthermore, to carry out experiments on non-mammalian vertebrates, there are fewer ethical issues involved. As a result, medical laboratories continually seek to replace mammalian models with animal models of lower phylogenetic classification [3].

Owing to its advantages, fish-based models are becoming increasingly important. However, there is an area of research in which fish are rarely used, which is medical imaging [3]. Among the few studies found, the medical imaging techniques used in zebrafish are Computed Tomography (CT), Radiography, Ultrasonography, and Magnetic Resonance Imaging (MRI). Nevertheless, the main goals of using these images are anatomic studies [3]. Whereas only a few studies are using the modality of Positron Emission Tomography (PET) in fishes. Few studies exist mainly because PET exams have to be realised *in vivo*, so it is imperative to maintain the zebrafish healthy and stable during the exam and do this without affecting the results.

In this regard, the current project focuses on studying the zebrafish (*Danio rerio*) as a model to study human diseases and responses to drugs used in their treatments, using the PET technology. The main goal of this work undergoes by the development of an enclosure capable of monitoring vital zebrafish signs and ensuring that environmental conditions remain stable during the PET image acquisition *in vivo*.

The experimental setup has an enclosure with a bed to comfortably accommodate the zebrafish. It also has sensors to monitor the fish's heart rate and measure the water temperature, ensuring the well-being of the animal. Therefore, the results presented in this project

intend to demonstrate the applicability of the zebrafish vital condition monitoring system during image acquisition and its potential to be applied in other areas of investigation.

So, the present dissertation is divided into eight chapters. The first and the second chapter expose the importance of the zebrafish as an animal model. The third one briefly explains how the PET technology works and highlights some medical imaging studies already performed with zebrafish. The zebrafish preparation for studies is presented in the fourth chapter. Then, it is explained how the zebrafish enclosure was built, from designing the enclosure to the monitoring system, in the fifth chapter. In the following chapters, the acquisition environment and the measurements of the zebrafish vital signs are described and discussed. Finally, the last chapter presents the work's conclusion and future improvements to the system.

Chapter 2

Zebrafish as an animal model

The zebrafish (*Danio rerio*) aroused the interest of the researchers in 1930. They were mainly used as a classical developmental and embryological model. Early studies combined the optical clarity of the embryos and their ease of handling to make *in vivo* observations of the cell-biological events [4]. Late in the 80s followed the implementation of genetic techniques in zebrafish, including cloning, mutagenesis, and transgenesis. In the 90s, it was possible to identify thousands of early developmental zebrafish mutants through genetic screens, establishing zebrafish as a mainstream model in development biology [4]. At this point it became important to understand the relation between the human and zebrafish genome to help identify the function of specific human genes from zebrafish mutations and zebrafish models for genes identified by human diseases. Reports from these studies pointed out the mapping of 124 zebrafish genes that are human genes orthologs [5] (around 70% of human genes can be found on zebrafish), highlighting significant parallels between both genomes.

Nevertheless, before understanding the full potential of zebrafish as an animal model to comprehend human development, diseases, and taxonomy, firstly, knowledge of the anatomy and physiology of the zebrafish must be developed. Thus, below it will be detailed the localisation and function of the zebrafish's main organ systems (Figure 2.1 a)).

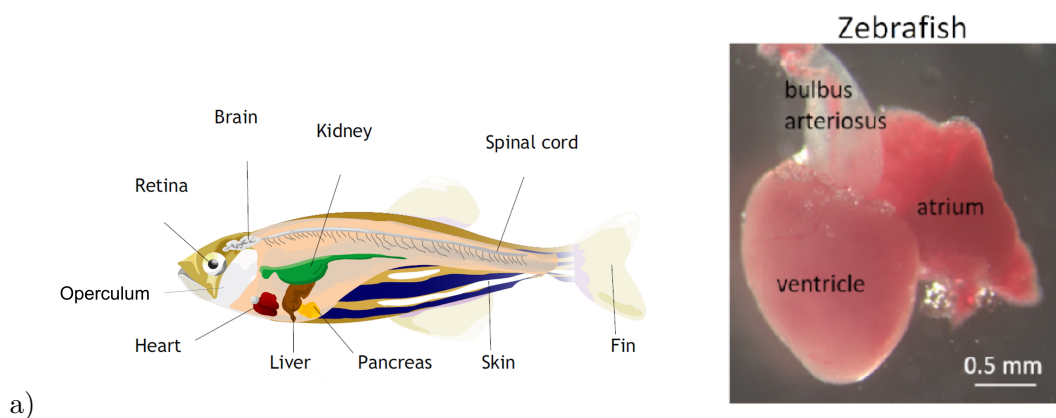


Figure 2.1: a) Anatomy of adult zebrafish. Adapted from [6]. b) Anatomy of the zebrafish heart. Adapted from [7].

The zebrafish's essential brain components are similar to those found in mammals and can be divided into five regions: the telencephalon, the diencephalons, the mesencephalon, the metencephalon, and the myelencephalon [8]. Besides, the zebrafish has all the main neuro mediators' systems, including neurotransmitters (such as GABA, glutamate, dopamine, nora-drenaline, serotonin, histamine, and acetylcholine) and enzymes of synthesis and metabolism homologous to those found in humans and rodents [9][10]. Furthermore, zebrafish also possess well-developed functional neuroendocrine systems like those observed in mammals. One example is the similarity, in the stress response, between humans and zebrafish, which is mediated by cortisol activated by cascade by hypothalamus-pituitary hormones and acting via glucocorticoid receptors [10].

The exocrine pancreatic tissue of zebrafish can be observed scattered throughout the intestinal tract (Figure 2.1 a)), and its acinar structure is very similar to that of mammals. The zebrafish's endocrine pancreatic tissue also has an evident resemblance with the mammalian's pancreatic cells. It includes the α -cells, responsible for producing glycagon-like peptide, β -cell, which produces insulin, and δ -cells, that produce somatostatin [8].

The zebrafish's liver can be divided into three lobes along the intestinal tract (Figure 2.1 a)). Like mammalian's liver, the main functions of zebrafish's liver are to maintain metabolic homeostasis of the body, which includes the processing of carbohydrates, proteins, lipids and vitamins, and detoxifying the body. The most evident difference between the zebrafish and mammalian liver is that hepatocytes are not organised in cords and lobules [8].

The crucial role of zebrafish's kidneys is to excrete water and maintain osmoregulation once they are freshwater fish [11]. However, there are similar structures between zebrafish and mammalian kidneys. Both have nephrons with a glomerulus, proximal tubules, distal tubules, and collecting ducts. The zebrafish kidneys are located in the ventral region of the vertebral column [8].

Relatively to the zebrafish gills, these have the essential role of oxygenating the blood. In this process, the water passes through the mouth, over the gills and out through the operculum. The alternate expansion and contraction of the opercular chamber drive the water flow [8].

The zebrafish's heart is positioned anterior of the main body cavity and ventral to the oesophagus (Figure 2.1 a)). In contrast to the mammalian's heart, the zebrafish's heart has a regenerative capacity, which aroused the interest of researchers [12]. Anatomically, the heart of the zebrafish differs from the human heart (which is made up of 4 divisions) due to its minimal size (100 times smaller) and because it consists of only two structures, only an atrium and a ventricle [7] (Figure 2.1 b)). However, zebrafish's heart has identical pumping mechanisms to mammals' hearts at cellular and molecular levels [13]. Physiologically, the deoxygenated venous blood enters the venous sinus and passes directly through the sino-atrial valve into the atrium. Afterwards, the atrium contraction and the ventricle dilation force the blood into the ventricle via the atrioventricular valve [8]. Then, the blood passes through the ventricle into the aorta [13]. Finally, the aorta distributes the blood to the gills via the afferent branchial arteries [8]. Also, the embryonic zebrafish heart rate rounds the 140 - 180 bpm, being much closer to the human fetal heart rate (130 - 170 bpm) and much slower compared to mouse heart rate (300 - 600 bpm) [13]. The basal heart rate of adult zebrafish is 120 - 130 bpm at 28 °C [14].

With this summary of zebrafish anatomy and physiology, it is possible to find some differences, like the lack of lungs. However, many organ systems, including the cardiovascular, the nervous, and the hematopoietic systems, are conserved between zebrafish and humans [15].

2.1 Influence of the environmental conditions

In the same way that it is essential to know the anatomy and physiology, it is also crucial to know and control the zebrafish environment conditions once these water quality parameters influence countless physiological aspects. More precisely, poor water quality can negatively affect growth, metabolism, development, immune system, behaviour, reproduction, and stress [16]. Therefore, the most critical parameters in water quality monitoring are: temperature, pH, dissolved oxygen, conductivity, alkalinity, hardness, ammonia (NH_3), nitrate (NO_3^-) and nitrite (NO_2^-) (Table 2.1).

Table 2.1: Optimum range of environmental water parameters for zebrafish.

Parameters	Ideal conditions	Reference
Temperature	24 - 29 °C	[17]
pH	6.8 - 8.0	[16]
Conductivity	200 - 3000 μS	[17]
Alkalinity	50 - 150 mg/L CaCO_3	[16]
Hardness	50 - 100 mg/L CaCO_3	[16]
Un-ionized Ammonia	≤ 0.02 mg/L	[16]
Nitrite (NO_2^-)	≤ 0.1 mg/L	[17]
Nitrate (NO_3^-)	≤ 50 mg/L	[17]
Dissolved Oxygen	6.0 - 8.0 mg/L	[17]

Most fish are poikilotherms which means the body temperature is adjusted to the environmental temperature around them. As such, the water temperature in the tank has the most significant impact on water quality. Furthermore, fluctuations in fish temperatures influence its growth, development, metabolism, physical activity, reproduction, and immunity [17]. Therefore, it will be necessary to regulate and control the water temperature in the tank of the zebrafish during the study. Zebrafish can tolerate a wide temperature range (eurythermal); however, the ideal water temperature range for zebrafish is between 24°C and 29°C, being that in this range, the growth rate is more considerable.

High temperatures lead to an increase in oxygen consumption and an increase in the heart rate of the zebrafish, reflected in a reduction of the dissolved oxygen present in the water. On the other hand, the environment temperature influences not only the zebrafish balance but also other water quality parameters. For example, the total ammonia balance depends on both temperature and pH; in other words, an increase in water temperature leads to a balance change in the sense of ammonia non-ionised forms and more toxins [17].

Like other water quality parameters, pH stability is vital for the fish's health. The zebrafish's environment should be maintained with a pH between 6.8 and 8 [16]. Acute exposure to a low pH ($\text{pH} < 4$) or a high pH ($\text{pH} > 11$) results in excessive production of mucus covering the skin and gills of the zebrafish, consequently leading to the destruction of the respiratory epithelium, the loss of swimming balance, convulsive behaviour, and death. Notably, the higher the pH, the more difficult it is for fish to bind and transport oxygen [17].

The oxygen levels dissolved in the water must remain within the range stipulated as ideal for zebrafish (6.0 - 8.0 mg/L). Outside these limits, the zebrafish can get in a state of oxidative stress leading to changes at the levels of reactive oxygen specimens and, in a severe case, can lead to its death [18].

Relatively to conductivity, this describes the concentration of dissolved ions and salts (sodium, potassium, calcium, magnesium, among others) in freshwater. To maintain salt and water balance, freshwater fishes avoid drinking water, secrete amounts of urine, reabsorb useful salts in the kidneys, absorb useful ions from food intake, and transport actively sodium (Na^+), calcium (Ca^{2+}), and chlorine (Cl^-) into the body fluid [17]. However, the maintenance of osmoregulatory balance represents a high energetic cost that increases as the water deviates from the ideal concentrations. Long-term exposure to an environment with too high or too low ion concentrations has adverse effects. The fishes constantly fight to reach balance in the digestion and the salts and water losses, leading to increased energetic expenditure [17].

The alkalinity is defined as the concentration of titratable bases (HCO_3^- , OH^- , CO_3^{2-}) in a solution. It has an essential role in maintaining the ideal pH, avoiding any damage or stress to zebrafish [17].

Regarding the water hardness, this one is a measure of divalent ions, such as calcium (Ca^{2+}), magnesium (Mg^{2+}), ferrous iron (Fe^{2+}), strontium (Sr^{2+}), and manganous manganese (Mn^{2+}). These are essential in enormous physiological processes, including brain function, bone tissue formation, blood clotting, muscular function, neurologic function, and osmoregulation [17]. To this extent, when occurs a deviation in the water hardness regularity, these physiological processes are affected.

Finally, the nitrogenous wastes have an origin in metabolic processes. Ammonia (NH_3), nitrite (NO_2^-), and nitrate (NO_3^-) are some examples. Ammonia is excreted metabolically by fish, and its concentration should not be superior to 0.02 mg/L; above this it becomes toxic to the zebrafish [16]. The toxicity of the nitrite molecules appears when these are transported up to the gill epithelium and oxidise haemoglobin molecules reducing the oxygen transportation efficacy. A high concentration (greater than 0.1 mg/L) of this molecule can lead to asphyxiation or even death [16]. On the other hand, nitrate is less toxic than ammonia and nitrite, given less capacity to penetrate the zebrafish gills. However, nitrate in high concentrations is also toxic (higher than 50 mg/L) [16].

Despite the importance of all water parameters previously described, the study realised in the present dissertation will only evaluate the dissolved oxygen, the pH, and the water temperature once these parameters require a more regular monitorisation.

2.2 Emerging fields of research

With both the knowledge about the anatomy and physiology of zebrafish and the ideal range of values of the water quality parameters for zebrafish, the characteristics that make zebrafish an essential animal in biomedical studies can be presented. In the last decades, the zebrafish rapidly emerged as an important animal model for investigations in enormous fields, like molecular biology, development biology, neurobiology, and genetic research [19]. Moreover, despite the apparent differences between zebrafish and human physiology, zebrafish offer countless advantages that make them a useful complementary model of mammalian diseases' models. As such, in Table 2.2, some evident advantages are shown.

Table 2.2: Main advantages of the zebrafish models in different areas of research.

Advantages of the zebrafish models	Observations
Short life cycle	Allows large-scale studies at a reduced cost and in a short period of time [20].
Simplicity of large-scale breeding	
Low maintenance costs	
Natural tissue regeneration capabilities	Attractive feature for areas such as evolutionary biology and regenerative medicine [6].
Optical transparency of embryos	Allows the initial development of images <i>in vivo</i> using microscopy techniques [20].
Sequenced genome	Allows conducting studies of genetic manipulation [4].
Lower phylogenetic classification (when compared with mammals)	Allows a reduction in the use of mammals in research, and there are fewer ethical problems associated [3].
Capacity for non-invasive drug administration	Ability to absorb substances dissolved directly in water through the gills quickly [21].

The combination of the unique characteristics of zebrafish proves to be extremely attractive in different areas, from cancer research to screening new drugs. This way, from a clinical perspective, the most productive contribution of the zebrafish as animal models passes by drawing pharmacology models and human diseases' models [4].

The genome sequencing of zebrafish, the capacity of reproduction on a large scale, and the short life cycle make the zebrafish models ideal for genetic studies once they allow genetic manipulation. Consequently, it allows identifying the genes responsible for the human disease and easily understanding the basic cell-biological processes that underline the disease phenotype beyond that gained from existing models [4], enabling the discovery of new treatments. One example passes by marking cell types involved in the infection and inflammation processes, which facilitates studying the processes that underline the disease progression [4].

Based on studies, zebrafish are also used to develop new therapeutic agents in new drug

research programs. Thus, drug tests conducted in zebrafish identify new component classes and their biological effects or redirect existing drugs to new applications [21]. However, the small size of zebrafish remains a challenge to quantify the internal exposure to the drug.

Due to the current empirical approach to nanomedicine and the countless variations in composition, shape, size, surface charge, and surface modification of nanoparticles, this area would undoubtedly benefit from an *in vivo* animal model, like zebrafish. Indeed, recent studies have been shown the true potential of zebrafish as an available tool for nanomedicine development [21]. The toxicity, biodistribution, stability, functionality, and targeting efficiency associated with nanomedicine have been successfully evaluated using *in vivo* zebrafish [21]. Relatively to biodistribution, the nanoparticles have been used to assess the tissue penetration and its capacity to cross the Blood-Brain-Barrier (BBB). Regarding functionality, nanoparticles containing drugs that are triggered through photothermal stimulation have been developed. Additionally, the nanoparticles can detect cancer cells and inhibit tumour growth, helping in cancer treatment.

Even though more than 300 million years separate the last common ancestor of fish and humans, cancer biology remains pretty much the same in these two species. The similarity is supported by comparing the human genome and the zebrafish genome. In both species, there are conservations of cell-cycle genes, tumour suppressor genes, oncogenes, genomic instability, invasiveness, transplantability, and the existence of cancer stem cells [21] [22]. In this regard, zebrafish are used to study various cancers' physiology by developing different transgenic cancer models. Some cancer studies using zebrafish are melanoma, pancreatic cancer, leukaemia, hepatoma, and rhabdomyosarcoma [21]. One specific example consists of using a zebrafish strain with a tumour suppressor gene mutation to find a second gene, which, when inactivated, prevents cancer formation [22].

Regarding immune system studies, rodents are the most recurrent model due to a wide range of knowledge and biological and molecular studies of their cells, which have been accumulated over the last few decades. However, rodents' biological aspects are a limitation; one example is the difficulty of recognising relevant embryonic lethal phenotypes [4]. For this reason, emerged the need to find an approachable genetic system, like zebrafish, which have an adaptative immune system that allows the research of the genes involved in host defence mechanisms [4].

Moreover, the study of complex brain diseases using zebrafish models has been increasing exponentially. Unlike rodents, zebrafish exhibit an intense neurologic activity throughout the brain and an impressive ability for brain repair during adulthood. Remarkably, these capabilities are possible due to the persistence of neural stem cells, including radial glia and neuroblasts [23]. Besides this, it was found that some pharmacological agents that modify synaptic transmission and neural membrane stability in humans reproduce similar activities in zebrafish, suggesting the existence of similar neural networks in these organisms [4]. These characteristics allow the study of various neurologic diseases using zebrafish models. Some examples of well-established diseases are anxiety and depression because, experimentally, the zebrafish can be easily exposed to various stressors, like chasing, crowding, disturbance of the light, changes in pH, restraint stress, or social isolation [24]. Other examples less recognised are addiction-related models, models of autism, and obsessive-compulsive states [24].

Other emerging fields of research that use zebrafish models are metabolic disorders, like

obesity and diabetes [23] because they are simple to manipulate and to set up an experiment, and cardiovascular diseases, since the zebrafish heart presents an analogous structure to mammalian hearts [25], and a robust regenerative capacity [12]. In addition, the characteristics of zebrafish heart allow them to be used as a human cardiovascular disease model and to be used to study damage of myocardial tissue caused by prolonged ischemia and hypoxia, which is typical myocardial infarction and the leading cause of heart failure [13].

In this way, it becomes evident that pre-clinic and clinic studies using zebrafish are essential for developing new therapies and discovering new biological mechanisms.

Although the zebrafish models present countless advantages and applications, there are some limitations associated with these models. For example, zebrafish do not have some organs present in humans (like skin, lungs, and prostate) reflected in their relative distance in the evolutive tree [20].

2.3 Anaesthesia

In general, to conduct experiments on adult zebrafish, it is necessary to sedate and immobilise them, so a good anaesthetic should be chosen. In studies using zebrafish, the most used and well-established anaesthetic is tricaine methanesulfonate (MS222). It eliminates muscle action potentials and spontaneous contractions (including sensory inputs and reflexes), so it works as a muscle relaxant [26]. However, this anaesthetic has some side effects such as: increases blood glucose, plasma cortisol, lactate, and blood chemistry values [27], reduces heart rate, which increases the risk of accidental death during anaesthesia. Consequently, other alternative anaesthetics have been studied. Some examples are lidocaine hydrochloride, metomidate hydrochloride, isoflurane, clove oil, gradual cooling.

When talking about anaesthesia of small animals, it is necessary to identify discomfort and pain by behavioural observations. Several signs make it possible to differentiate between a normal and distressed state. In zebrafish, some signs are an excessive movement of the opercula (hyperventilation), cough rate (reversal of water flow direction over the gills), colour (pigmentation) changes, and increased movement (hypertaxia) or cessation of movement (ataxia) [26]. Besides, the anaesthesia levels can also be characterised by several behavioural criteria, some of which are described in Table 2.3.

The study [27] compared the efficiency and safety of several anaesthetics, like gradual cooling, lidocaine hydrochloride, and metomidate hydrochloride, and isoflurane with MS222 for anaesthesia of adult zebrafish. Gradual cooling proves to be useful for immobilisation. However, it is challenging to maintain the fish at these conditions for prolonged procedures because they appeared to recover as soon as they came into direct contact with room temperature instruments or surfaces. So gradual cooling is not recommended for invasive procedures, and it is not an effective anaesthetic per se. Metomidate hydrochloride was only able to reach the level of sedation. Isoflurane has been proven to induce distress in all fish, resulting in high mortality rates. Zebrafish achieved a plane of surgical anaesthesia faster with lidocaine hydrochloride, but recovery was longer than that for MS222, and a high dose of this agent caused high mortality levels. Thus, this study concluded that lidocaine hydrochloride and isoflurane alone were not suitable to anaesthetise zebrafish. Therefore, MS222 remains the best choice for inducing a surgical plane of anaesthesia. So, in the present dissertation, it was

used MS222 to anaesthetise zebrafish.

In Table 2.4, it is shown the influence of different anaesthesia and concentrations. Observing the data provided in Table 2.4, it is possible to notice that the higher the anaesthesia concentration, the lower is the zebrafish heart rate. In addition, with the course of the study, the heart rate decreases even more. Moreover, the heart rate of the anaesthetised zebrafish is lower than its basal heart rate.

Table 2.3: Stages of anaesthesia and the consequent effect in several behavioural criteria. (Adapted from [27]).

Stage	Level	General behaviour	Equilibrium	Rate of operculum movement	Reflex response	Heart rate	Muscle tone
0	None	Normal	Normal	Normal	Normal	Normal	Normal
I	Sedation	Disorientation	Difficult to maintain	Normal	Reduced	Normal	Normal
II	Excitation	Agitation	Lost	Increased	Increased	Increased	Normal
III - 1	Light anaesthesia	Anaesthetised	Lost	Decreased	Reduced	Regular	Decreased
III - 2	Surgical anaesthesia	Anaesthetised	Lost	Shallow	None	Reduced	Decreased
III - 3	Deep	Anaesthetised	Lost	Rare movements	None	Reduced	Relaxed
IV	Overdose	Apparently dead	Lost	None	None	Cardiac Failure	None

Table 2.4: Influence of different anaesthesia and different concentrations on the zebrafish heart rate.

Reference	Anaesthesia	Heart Rate	Technique used to detect the heartbeat
[28]	MS222 200 mg/L	(Mean) 118 ± 14 bpm	Surface ECG
[14]	MS222 392 mg/L	72 ± 14 (1 min), 72 ± 12 (3 min), 71 ± 11 (6 min), 63 ± 10 (9 min).	Standardised ECG
[14]	MS222 196 mg/L	125 ± 10 (1 min), 122 ± 10 (3 min), 106 ± 11 (6 min), 96 ± 8 (9 min).	Standardised ECG
[29]	AQUI-S 3 mg/L	120 ± 10 (1 min), 124 ± 11 (3 min), 110 ± 8 (6 min).	Light-cardiogram
[29]	AQUI-S 3 mg/L	88 ± 14 (1 min), 74 ± 12 (3 min), 69 ± 10 (6 min).	Light-cardiogram

Chapter 3

Imaging techniques used on zebrafish

As shown in the previous section, zebrafish studies contribute to the evolution and discoveries in biomedical research. Notably, images of the zebrafish can provide the means to address non-invasive monitoring of biological processes, disease progression, and response to therapy, with the potential to provide a natural bridge to the clinic environment and contribute substantially to the development of human medicine [30]. However, there are few diagnostic and monitoring systems and technologies for these small animals.

Therefore, this chapter presents a brief explanation of the PET functioning and some studies conducted in zebrafish using this imaging modality. Besides, other imaging techniques applied to zebrafish and also their relative limitations are exposed.

3.1 Positron Emission Tomography

Nowadays, there are image techniques to access the anatomic characteristics of zebrafish, like CT and MRI . However, there is not much evidence on the realisation of functional imaging modality, PET, *in vivo* in zebrafish [3]. The main reason is that there are several obstacles to progress in this area, such as the small size of zebrafish (2 - 4 cm) relatively to the spatial resolution typically achievable with PET , nowadays close to 1 mm, making it challenging to design an enclosure capable of immobilising them during the exam period and in the aquatic environment. Also, the physiological requirements of zebrafish, which demand vital signs and environment quality monitoring equipment waterproof, and the zebrafish immobilisation to avoid any movement during the exam are obstacles to conduct PET exams on zebrafish. In this way, the present work aims to develop a system capable of overcoming the difficulties of performing a PET exam on a zebrafish *in vivo*.

3.1.1 Physical principles

PET is a diagnostic technique widely used in nuclear medicine. In this technique, a radiotracer is administered to a patient. This radiotracer is a chemical compound with

interest in physiological processes linked to a radioisotope. It is distributed according to the patient's physiological state, capable of detecting changes at a molecular level [31]. The radiotracer is carefully chosen according to the biochemical or metabolic process that will be studied and evaluated.

During the PET exam, the unstable radioisotopes undergo decay and emit positrons through beta decay. This positron travels a short distance and collides with electrons present in great abundance in the human body, resulting in an annihilation reaction. In this reaction, both positron and electron masses are converted into energy by emitting a pair of gamma photons in opposite directions (approximately 180°) and with well-defined energy (511 keV) [31] (Figure 3.1).

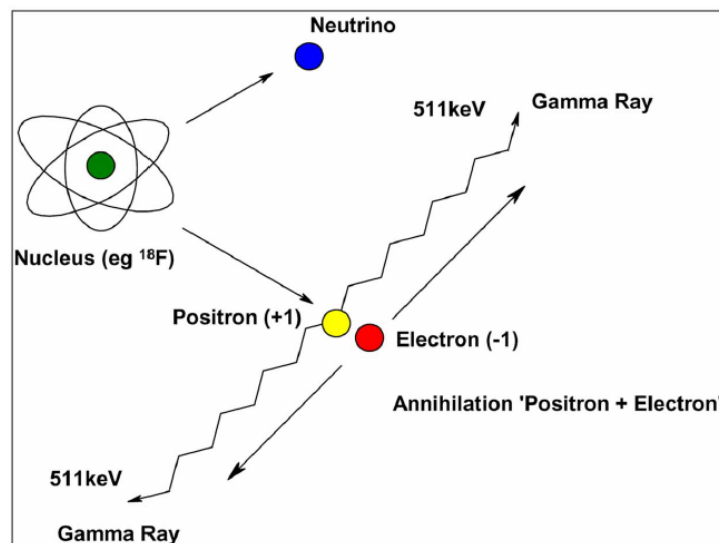


Figure 3.1: Diagram of the positron emission during the decay process of a radionuclide and the annihilation process. Adapted from [31].

The gamma rays leave the patient's body and are detected in coincidence by a ring system of detectors surrounding the patient's bed (Figure 3.2). This distribution allows that one pair of detectors detects two photons in coincidence in any direction. After that, these signals are reconstructed, and possible errors are reduced, such as attenuation, scattering, and random coincidences [32]. The resulting images show the radioactivity concentration on the target tissue (Figure 3.2).

After being emitted and before reaching the detector, the gamma radiation can interact with the body in different ways, essentially by photoelectric absorption, Compton scattering, and pair production. These phenomena are significant and must be considered in the PET image reconstruction algorithms since the photon interaction with the medium can cause detection errors.

The reconstruction procedure of a PET image consists of simultaneous detection of two gamma photons of 511 keV, by two detection cells, within a sufficiently small-time window (typically below 10 ns) defined by the resolution of the system. This event is called true coincidence. Thus, it is assumed that the trajectory of the two photons is the line that

connects the two detection units, which is called the Line of Response (LOR) [33] (Figure 3.3). However, it is impossible to know the exact position where the annihilation occurred along the LOR by detecting only a single event. The repetition of this process for all detected events allows the drawing of different LORs. Consequently, the overlap on an image highlights a region with a high density of LORs, representing the most probable distribution and higher concentration of the radioactive material [34]. So, the spatial distribution of the radioisotope is obtained from the intersection of all LORs, and the final image usually is reconstructed using iterative algorithms and filtering techniques.

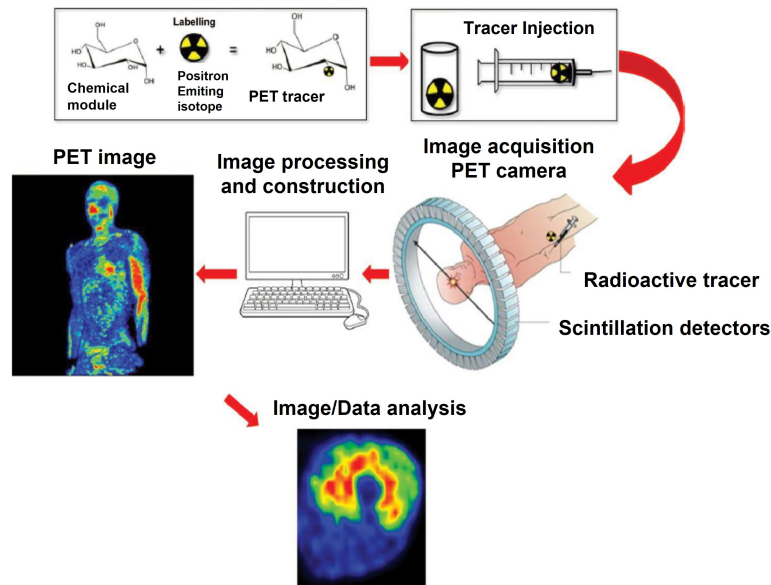


Figure 3.2: Process of the PET image acquisition. Adapted from [35].

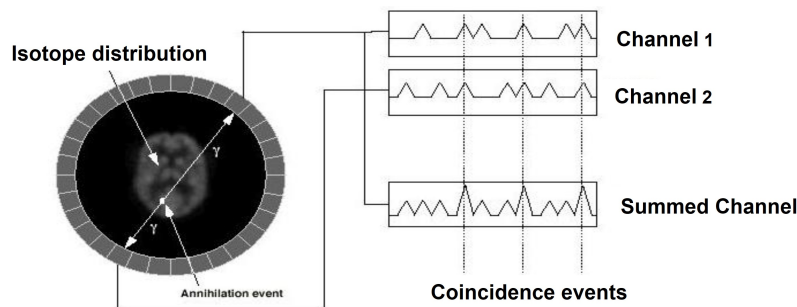


Figure 3.3: Representative scheme of the signals acquisition from an annihilation event. Adapted from [33].

However, due to the influence of some physical phenomena, different events can occur, such as random and scattering coincidences (Figure 3.4). In a random coincidence, two photons with origin in different annihilation processes are detected within the same time window, creating an incorrect LOR. In the scattering events, at least one of the photons from the same annihilation event suffers Compton scatter before reaching the detector [36]. As a result, the LOR does not pass by the local where the annihilation occurred. The

scattering and random events are unwanted since they are noise sources whose primary effect is reducing the image contrast and resolution [33].

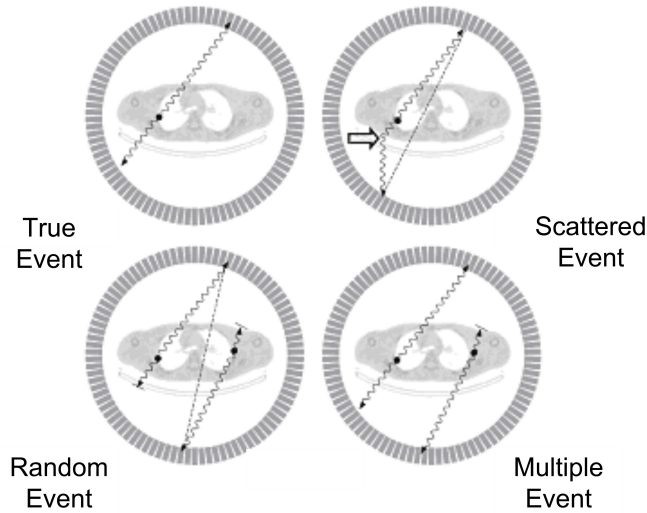


Figure 3.4: Physical phenomena that can occur from annihilation to detection (during the acquisition of PET images). The black dots indicate the position of the annihilation of the positron with the electron. Adapted from [37]

3.1.2 Studies with zebrafish models

Considering both the PET technology characteristics and the studies that have currently been conducted on zebrafish, its combination can result in numerous advantages and research applications. Hence, it can enhance non-invasive and more effective monitoring of the disease progression at the molecular level, as well as new therapy forms. Additionally, it enables analyses over time to evaluate the disease progression and define the pathology nature [4]. Other areas of interest are the inflammatory processes. PET allows tracking the inflammatory response triggered in transgenic zebrafish [4], the cancer monitorisation, and the brain activity of zebrafish in real-time and *in vivo*. Lastly, the zebrafish reveals regenerative capacities in various organs, particularly in the heart. However, it has not yet been possible to understand how cardiac cells are successfully used in regeneration and how the epicardium is activated and oriented to support regeneration [12]. In this sense, PET technology can monitor the entire regeneration process at the molecular and functional levels, increasing knowledge about the regeneration mechanisms, bringing the idea of cardiac regeneration in humans closer to reality.

However, once zebrafish presents a reduced size, which implies that its organs are also tiny (a few millimetres), it is necessary to use pre-clinic PET systems. For instance, the present work was idealised in the scope of the easyPET system, a pre-clinical PET system based on a single pair of collinear detectors that rotate around the centre of the system, reproducing, this way, the same effect as in a conventional PET detectors. This way, once the easyPET system has fewer components when compared with conventional PET systems, its cost is also reduced. Besides, compared with other pre-clinic systems, the easyPET system

has a high spatial resolution (close to 1 mm) but with less sensibility, which needs to be compensated with the increase of time acquisition. [35].

Moving to a more detailed explanation of how the PET exam is conducted in zebrafish, this section presents the protocols and results of three different studies. The first one investigates which medical imaging techniques are compatible with zebrafish [38]. The second aims to define acute and chronic models of hyperglycemia in zebrafish throughout the monitorisation of radiomarked molecules using PET /CT [23]. The last one compares two medical imaging techniques, PET and Desorption Electrospray Ionisation - Mass Spectrometry (DESI-MS), in a zebrafish melanoma model [39].

The first study [38] used the *Bruker Albira* equipment for the 3D imaging modalities. The PET scan tested two radiotracers, ^{18}F -FDG (*2-Deoxy-2- ^{18}F fluoroglucose*) e ^{18}F -NaF, and were injected into different fish tanks with an activity of 428 μCi and 480 μCi , respectively. The zebrafish were maintained in these environments for 45 min. For the image acquisition, the zebrafish were placed in the centre of the imaging platform and maintained there for 20 min (PET scan duration). Thus, the study was able to acquire images following this protocol successfully (Figure 3.5 a)).

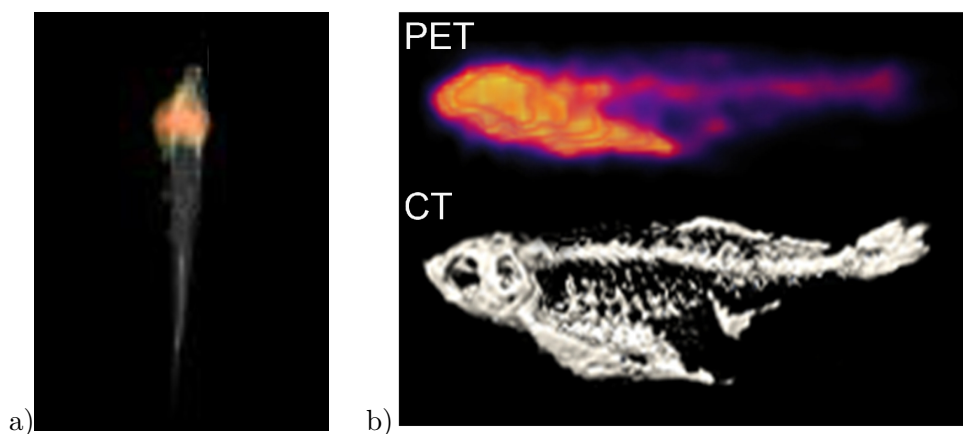


Figure 3.5: a) PET image of zebrafish 20 minutes after removing the fish from the tank with the ^{18}F -FDG . Adapted from [38]. b) PET /CT imaging of ^{18}F -FDG (20 MBq injected) 30 min after the intraperitoneal injection. Adapted from [23].

In the second paper [23], the zebrafish were anaesthetised with a tricaine solution (0.02 % concentration) and then injected in the intraperitoneal cavity with a saline solution of ^{18}F -FDG with 20 MBq activity. A radioisotope calibrator measured the remaining activity on the syringe and tissue to calculate the exact injected dose. Later, the fish was wrapped in a small piece of absorbent tissue soaked with tricaine and then placed in the bed of the PET /CT system to start acquiring images. After the scan, the fish was placed again in a tank with fresh water. Another alternative to this procedure was placing the zebrafish in a tank with fresh water after being injected with radiotracer ^{18}F -FDG for ten minutes to one hour. This alternative facilitated the radiotracer diffusion before anaesthetising the fish once again for PET /CT imaging. After 30 min, the PET /CT images showed that glucose is distributed at the injection site and in the zebrafish head (including the brain) and spinal cord. The protocol followed and the results described in this paper present a particular interest when it is intended to determine the bioaccumulation of a potential therapeutic agent in an *in vivo*

3.2 Other imaging techniques conducted on zebrafish

The growing scientific interest in zebrafish as a model organism in various biomedical and biological research raises the need to develop *in vivo* imaging tools suitable for this animal model. Therefore, this section exposes different approaches to perform medical imaging technologies adjusted to zebrafish and some gaps in these tools. So, three studies with different medical image modalities are approached, one about MRI [1], another that uses high-frequency ultrasound [25] and other about electrocardiography [7].

3.2.1 MRI

The MRI system is based on the article [1], whose goal is to develop a novel MRI coil and animal handling system optimised for high-resolution scanning of *in vivo* zebrafish. Being composed of a radio frequency micro-solenoid (RF) coil that is integrated into an animal handling system known as a flow cell (Figure 3.7). The flow cell was designed to minimise the diameter of the RF coil while keeping the zebrafish immobilised and comfortable. Also, the flow cell constantly provided water with dissolved oxygen and anaesthesia. Besides this, the enclosure used in this study has an environmental monitoring system to ensure that the animal remains physiological stable during the MRI scan. The water pumped into the system has a reduced flow rate (2 ml min^{-1}) to minimise flow artefacts in the MRI images. This system used a PT100 temperature sensor to measure the water temperature and an optical sensor to measure the dissolved oxygen. The zebrafish were anaesthetised with MS222 outside the system at a concentration of 125 mg/L. Only then it was placed into the flow cell, where they were held correctly in position. Inside the system, they were maintained with a low dose of anaesthesia (MS222 100 mg/L). The zebrafish inside the flow cell is held in place throughout tiny sponges and pieces of paper towel placed between the sides of the enclosure and the fish. After the correct positioning, the chamber is sealed, and all monitoring equipment and the water pump are turned on.

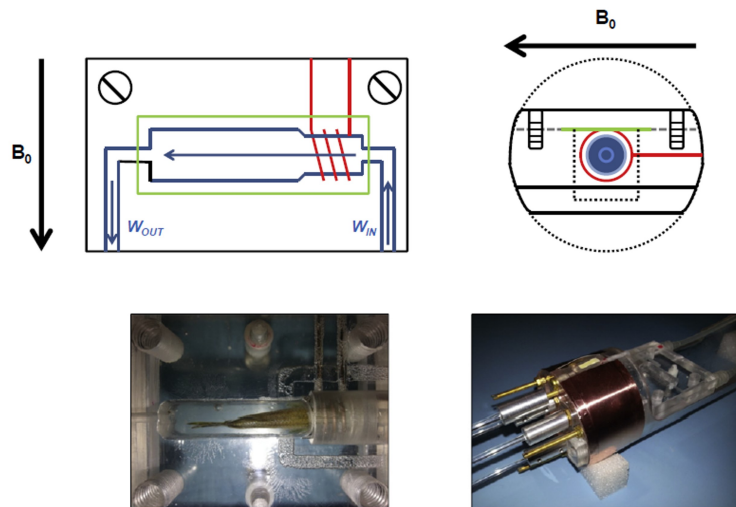


Figure 3.7: Zebrafish MRI flow cell system. Adapted from [1].

The results obtained with this study [1] were satisfactory once they managed to identify anatomic structures, like the gill, the eyes, the brain, the heart, the liver and the swim bladder. Regarding the duration to induce anaesthesia in zebrafish, it was verified that it only took two to three minutes. After the scan, the zebrafish demonstrated rapid recovery immediately after being placed in a tank with normal water, free from the anaesthetic. They did not show signs of injury or stress.

3.2.2 Ultrasonography

Another example of a medical imaging modality used in zebrafish is the high-frequency ultrasound, presented in the following paper [25]. This paper reports the development of an ultrasound system to investigate the adult zebrafish cardiovascular system, capable of generating 75 MHz B-mode imaging at a spatial resolution of 25 μm and 45 MHz pulsed-wave Doppler measurement. The zebrafish were anaesthetised before the exam by submerging them in a 0.08 % tricaine (MS222) solution for thirty seconds. Then, the scales from the ventral side between the gills were removed. Immediately after, the zebrafish were kept on a solution of 0.04 % tricaine throughout the exam. All the studies elapsed at 27.5 $^{\circ}\text{C}$ for less than twenty minutes. Each zebrafish, during the exam, was placed upside down in a small rubber holder inside a plastic container (Figure 3.8). The ultrasound probe was attached to a holder that descended until it was at a distance of 3 mm of the fish's skin. After the procedures, the animals were euthanised by placing them in a 1 % tricaine solution for fifteen minutes. So, the ultrasound system presented in this paper could trace cardiac structures in real-time and estimate their respective dimensions.

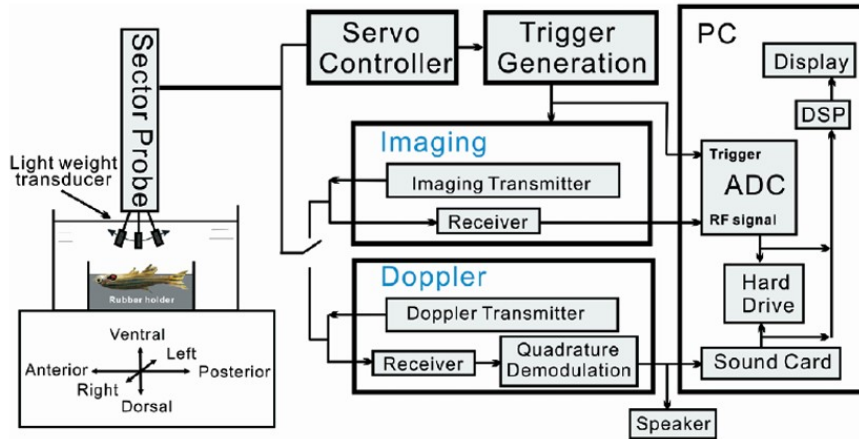


Figure 3.8: Block diagram of a high-resolution ultrasonic system for studying the cardiovascular system of an adult zebrafish. Adapted from [25].

3.2.3 Electrocardiography

A different approach to evaluate the zebrafish cardiovascular system is through electrocardiography. In this sense, paper [7] explains all the procedures to realise electrocardiography *in vivo* in adult zebrafish. In this study, it was necessary to anaesthetise the fish to minimise

pain and quickly immobilise them, avoiding any movements during the acquisition of the ECG signals (avoid motion artefacts). The anaesthesia protocol is identical to most of the studies that use zebrafish. It used one solution of 0.02 – 0.04 % tricaine, and the fish were immersed in that solution until they reached level four anaesthesia (approximately three minutes). As soon the fish reached that level, the zebrafish was transferred onto a damp sponge with the ventral surface upwards to enable the positioning of the electrodes (Figure 3.9). These ECG electrodes were gently inserted into zebrafish musculature to approximately 1 mm in depth. At the end of the ECG recording session, the zebrafish were transferred into a water recipient with dissolved oxygen and free from anaesthesia. Once the zebrafish could swim straight for at least five seconds, it was considered that it recovered from anaesthesia.

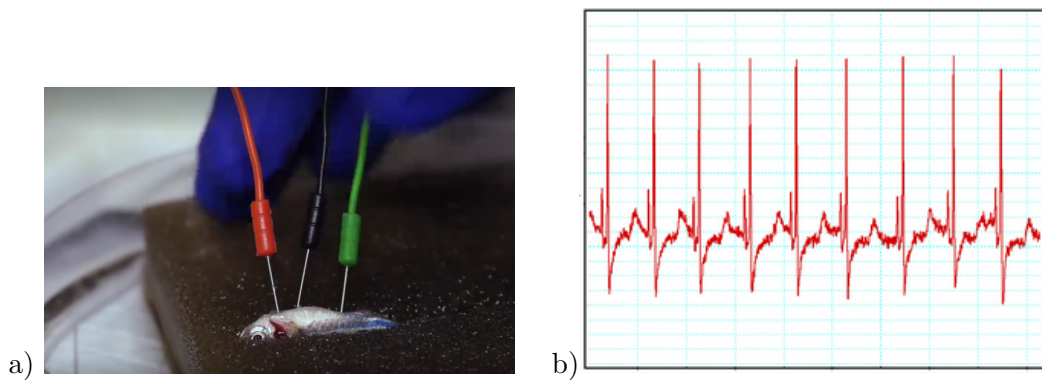


Figure 3.9: a) Immobilisation and positioning of electrodes for ECG acquisition in zebrafish. b) ECG obtained. Adapted from [7].

Chapter 4

Ethics and protocols for zebrafish preparation

The animals used for scientific purposes, including the zebrafish used in this study, were protected under the directive 2010/63/EU. In compliance with this directive, the principle of the Three Rs, to replace, reduce and refine the use of animals for scientific propose, was respected in this project. Accordingly, careful planning of the experimental design was done to decrease the chance of errors and unsuccessful experiments; an extensive literature review was also done on all topics involved to avoid unnecessary testing. Furthermore, the fish well-being was accessed at all stages of the experiments to minimise suffering, including anaesthesia administration and recovery. When needed, euthanasia was performed according to the methods approved by the competent entities. Moreover, this project was subjected to the ethics committee of the Biology Department of University of Aveiro, CREBEA (*Comissão Responsável pela Experimentação e Bem-Estar Animal*) and to the national competent entity DGAV (*Direção Geral de Alimentação e Veterinária*) for approval.

In the present work, it was necessary to define the protocol to prepare and maintain the zebrafish stable for the experiments. Therefore, the zebrafish used in this project were kept in tanks with adequate conditions (Table 2.1) in the bioterium of the Biology Department of the University of Aveiro. To carry out the experiments with zebrafish it was necessary to immobilise them using an anaesthetic. The anaesthetic chosen was MS222 . This substance is dissolved in water, forming a solution. However, as it is an acidic substance, it is necessary to neutralise the solution using a basic solution (sodium hydroxide, NaOH). Therefore, the NaOH solution was added until the anaesthetic solution pH reached between a value 7 and 8.

The protocol followed in the present work to anaesthetised zebrafish (Figure 4.1) was based on the paper [1]. Thus, it was needed to prepare two MS222 solutions, one with a 125 mg/L concentration and another with 100 mg/L. The anaesthetic process starts by emerging the zebrafish on the solution of MS222 with a higher concentration (125 mg/L), for about three to five minutes. The zebrafish remain on this solution until they reach a level of surgical anaesthesia (loss of equilibrium, no reflex response, and slower opercular movement). At this point, it was observed the different aspects of the fish's behaviour. The equilibrium loss was verified as soon as the fish remained upside-down with their ventral abdomen oriented toward the surface of the water for five seconds. Next, the reflex response was evaluated by applying

pressure in the tail fin with forceps, and if the fish is well anaesthetised will not have an observable reaction. Finally, the slowing of the opercular movement was easily observed by looking at the fish. The moment that it was verified that the zebrafish reached the surgical level of anaesthesia, this one was transferred to a solution with a lower concentration (100 mg/L). The solution with a lower concentration was used to maintain the fish under the effect of the anaesthesia. It was in this last solution that the studies of the present work took place. After the studies, the zebrafish were placed in a tank filled with fresh water to recover from anaesthesia. The recovery of the zebrafish was observed after three to five minutes exposed to freshwater.

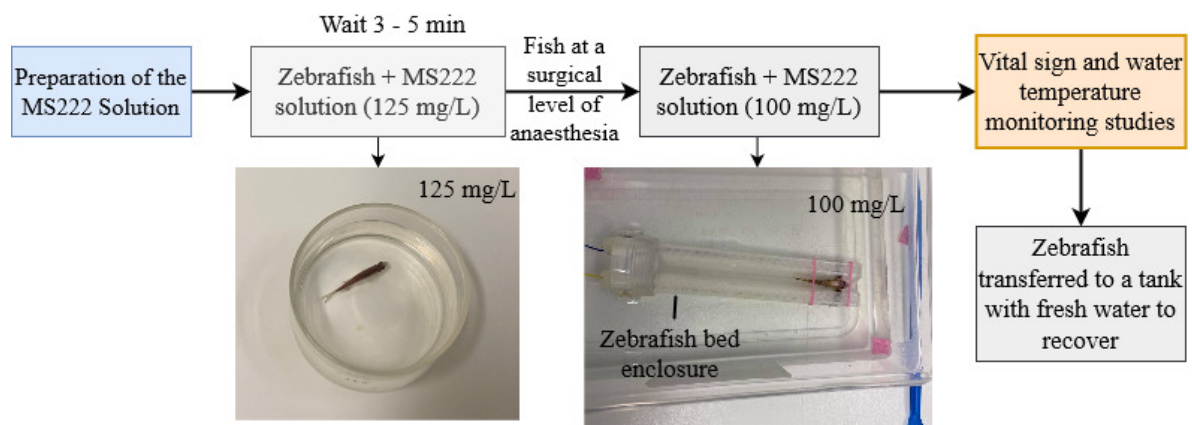


Figure 4.1: Anaesthesia protocol followed in the present dissertation.

Chapter 5

Zebrafish Enclosure

This chapter presents all the procedures followed for developing a zebrafish enclosure in order to obtain PET images *in vivo*, from the enclosure design to the system responsible for monitoring the zebrafish.

5.1 Design proposal

The enclosure developed consists of a closed chamber capable of aligning the zebrafish with the heartbeat sensors and immobilising them during the trials. Besides the heartbeat sensors, the enclosure also has a thermistor that measures the water temperature.

This enclosure is composed of two different parts, the zebrafish's bed (immobilisation block) (Figure 5.1 a)) and another that wraps around the immobilisation block (Figure 5.1 b)). This last component is used for maintaining the water in a closed container. This enclosure configuration was thought to facilitate the zebrafish placement in an horizontal position, preventing the fish from leaving the place and allowing an effortless closing of the container when filled with water.

In the enclosure designing process some characteristics were considered to improve the maximum quality of PET imaging. So, it was designed an enclosure with reduced dimensions to bring PET detectors closer to the animal, improving the PET image quality. Additionally, the material of the chamber should be transparent to enable the visualisation of the fish, ensuring that the animal does not exhibit signals of stress. Also, the material should have a reduced atomic number (water equivalent) to reduce the interaction with the radiation during the PET exam, improving the image's quality. Thus, the material chosen for the chamber was the polymer *Poly(methyl methacrylate)* (PMMA).

The immobilisation block is constituted by two parts, one made from PMMA and another manufactured using a 3D printer (zebrafish's bed), which made it easier to make adjustments during the study. These adjustments were made according to the results obtained in some experiments. In other words, the base made with PMMA was maintained with a fixed design since the beginning, while the printed piece was altered due to the constraints that emerged during the different tests performed. The different designs of all the parts were

developed using the SolidWorks [®]¹ tool. The PMMA piece that works like the support for the zebrafish's bed was built in the workshop of the Physics Department of the University of Aveiro. Also, the zebrafish's bed design was printed in the 3D printer of the Physics Department of the University of Aveiro.

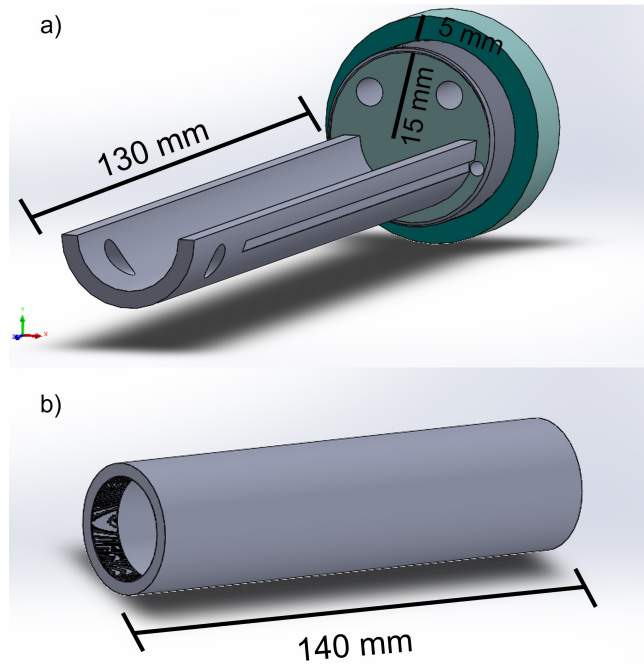


Figure 5.1: a) Design of the immobilisation block of the zebrafish's bed. b) Design of the cylinder that wraps around the immobilisation block, closing the container.

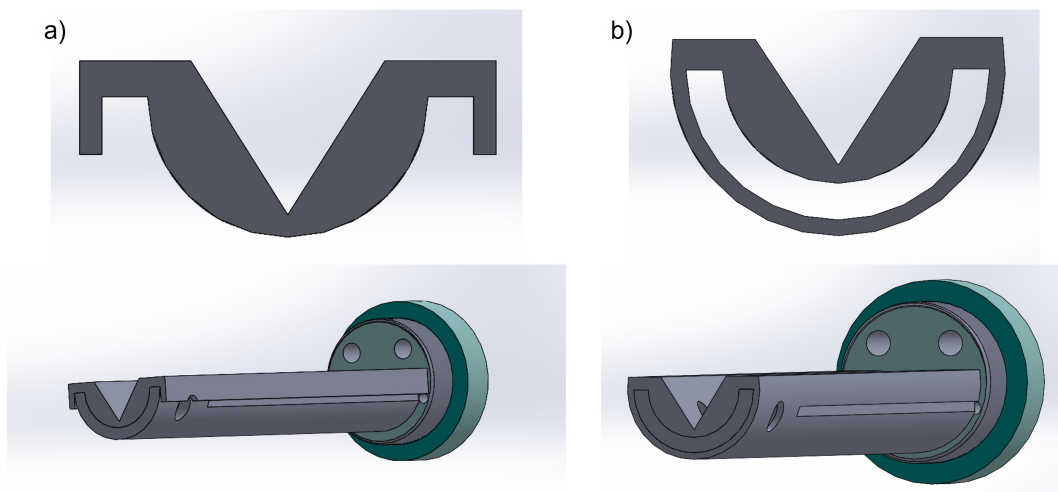


Figure 5.2: Design of two different bed prototypes. a) "V" shaped bed, with less volume and easier to place and remove the piece. b) "V" shaped bed, with more volume and more difficulty to place and remove the piece.

¹<https://www.solidworks.com/>

Initially, two pieces were printed with different designs (Figure 5.2) with a "V" shaped bed and circles to fixate the sensors. However, after doing some tests, it was realised that the "V" shaped bed does not immobilise the zebrafish adequately, and the sensors were located below the zebrafish heart region. Relatively to the general shape of the piece, the design chosen to maintain was the one presented in Figure 5.2 a) since it is easier to place and remove the piece and occupies less volume than the design of Figure 5.2 b). However, these two designs suffered some adjustments. The shape of the bed was changed to a trapeze (Figure 5.3 a)), and the holes for the sensors were expanded (Figure 5.3 b)). In the PMMA piece it was also necessary to cut the holes to enable the repositioning of the sensors. Besides the adjustments made in the bed of the zebrafish, it was necessary to use a sponge to immobilise them more efficiently, as illustrated in Figure 5.4. The sponge was cut so that the region where the zebrafish's head lies is broad, and the tail region is tighter to keep the zebrafish immobilised.

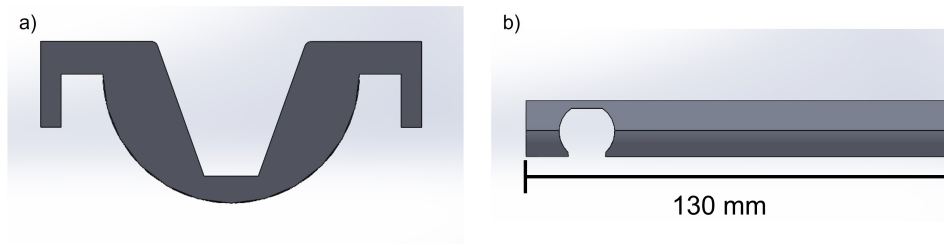


Figure 5.3: Upgrade of the design of the zebrafish bed. a) The bed shape changed to a trapeze. b) The sensor holes in the bed were expanded.

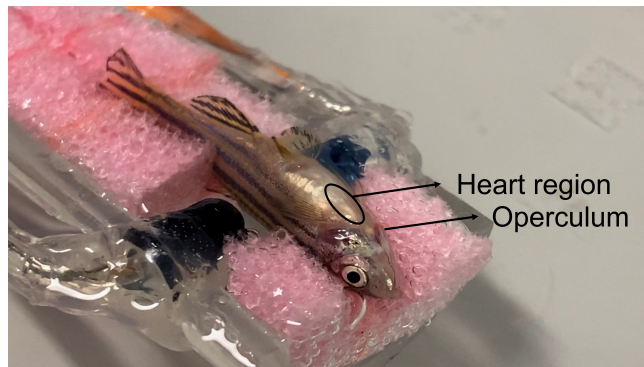


Figure 5.4: Zebrafish in the bed with a sponge to improve immobilisation.

5.2 Monitoring system

In the present work, a non-invasive system was developed to easily monitor the cardiac activity of zebrafish and water temperature.

This way, it is known that there is a change in blood volume with a heartbeat, so the intensity of an infrared light passing through a tissue depends on changes in the blood volume (heartbeat) circulating within the tissue. Also, the haemoglobin exhibits relatively high absorbance for infra-red light. Based on these principles, placing an infrared light emitter

on one side and another infrared light receiver on the opposite side of the body, it is possible to optically detect the pulse produced by the heartbeat, making it possible to monitor the heart's activity.

Therefore, the monitoring system built in this project is composed of a transmitter, an infrared light-emitting diode (IR LED), and a receiver, a phototransistor (optical sensor). These components were placed on opposite sides of the zebrafish body, as illustrated in Figure 5.5. The IR LED is responsible for sending infrared light towards the body, and some light is absorbed. This way, the optical sensor senses the change in blood volume and produces a signal. However, this signal is so small in magnitude that it cannot be detected directly by the microcontroller. Hence, the signal needs to be filtered and amplified. Only then, the signal is sent to the microcontroller, where it is processed and posteriorly sent to the computer, where a Python script determines the heartbeat.

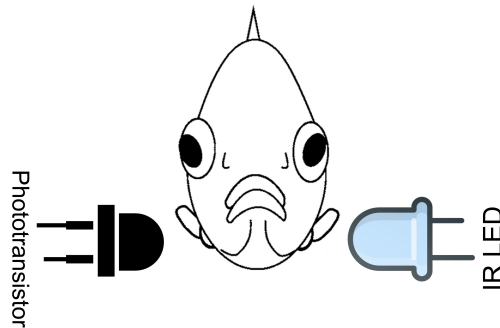


Figure 5.5: Sensor arrangement relative to the zebrafish (front view).

Besides the unit responsible for the heartbeat monitoring, it was also necessary to assemble a unit for the water temperature monitoring. The temperature sensor that was chosen for this application was a Negative Temperature Coefficient (NTC) thermistor. The thermistors are temperature sensors based on semiconductors, and the resistance between its terminals varies with the temperature. The NTC thermistors have the particularity of decreasing their resistance when the temperature increases, and because of this, the negative temperature coefficient comes up. These sensors have a non-linear response, yet they have the highest sensitivity in the low-temperature zone, hence the choice for this application.

For a better understanding, Figure 5.6 represents a block diagram that describes the hardware and software of the system and its connections, providing a functional view of the whole system. As shown in Figure 5.6, the sensors are underwater in the same environment as the zebrafish. First, the signal produced by them is filtered and amplified in the conditioning circuit. Then, the microcontroller reads and converts the signal to a digital number and sends these data to a Python program. Finally, the data is processed and displayed in a Graphical User Interface (GUI).

Furthermore, throughout the tests became necessary to add a camera (*Webcam Logitech Quickcam USB V-UAR38*) to record the experiments and validate the data acquired by the sensors.

Next in this section, the heartbeat conditioning circuit, water temperature conditioning circuit, firmware and software used to build this system are exposed in more detail.

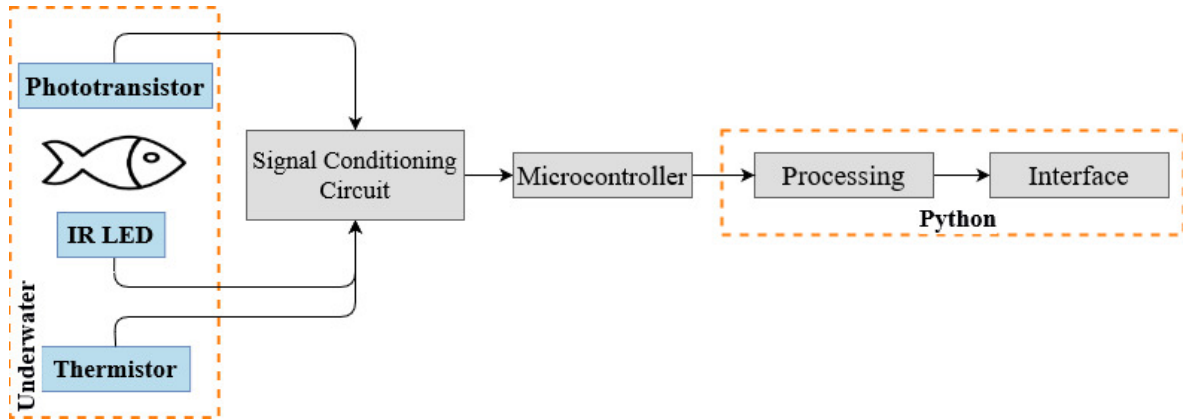


Figure 5.6: Block diagram of the heartbeat and water temperature measurement and display.

5.2.1 Heartbeat conditioning circuit

Relatively to the zebrafish heartbeat detection system, an IR LED (*TSAL6100*, Vishay Semiconductors, peak wavelength 940 nm) and a phototransistor (*L-53P3C*, Kingbright, supports 940 nm wavelength) were used. They were placed on opposite sides, aligned with the zebrafish heart (located behind and below the gills). The IR LED is powered with +5 V by an Arduino UNO R3. The IR LED state is also controlled by a digital signal sent by an Arduino analog port (A0) and driven by a transistor BC547B. There is a change in the blood volume with a heartbeat, so there is a variation in the absorbed light. Consequently, the phototransistor senses the light levels and alters the current flowing between the emitter and collector according to the level of light it receives. This signal is so small in magnitude that it is necessary to amplify and filter it, which is accomplished in the signal conditioning circuit.

In this project, for the conditioning of the signal produced by the phototransistor, it were designed two different circuits interconnected with a shared stage (Figure 5.7 a)). Therefore, two different signals (A1 and A2) are obtained at the output of the circuits. However, in both circuits, the output signal from the phototransistor is converted into a suitable and usable quantity that will be ready for processing later.

At the shared stage, the signal produced by the phototransistor passes by a capacitor of 1 μF to block the Direct Current (DC) component in the signal. Then, the amplification of the signal is done by using an *LM358* operational amplifier. The *LM358* consists of two independent, high gain and frequency compensated operational amplifiers (OPAMP 1 and OPAMP 2). At the shared stage, the first operational amplifier (OPAMP 1) is used in a non-inverting mode, and the gain is 101 ($G1 = 1 + \frac{R6}{R5} = 1 + \frac{680k}{6.8k} = 101$). Besides the amplification, the signal also requires filtering. The signal is affected by interference resulting from the movement of artefacts and mains 50 Hz. Thus, the filtering is done by using a simple resistor and capacitor. They are arranged to act as a low pass filter (cutoff frequency of 2.34 Hz) and block higher frequency noise components present in the signal.

At the output of the OPAMP 1 arise the differences in the circuit between the two signals. The A2 signal is produced by applying a simple low pass filter to the OPAMP 1 signal output. This filter has a cutoff frequency of approximately 10 Hz. On the other hand, for the

A1 signal, the OPAMP 1 signal output passes by another stage of amplification and filtering. The filtering components are a resistor and a capacitor that form a high pass filter with a cutoff frequency of approximately 1 Hz. This filter is responsible for blocking the DC component that might exist. For the amplification, it has another operational amplifier (OPAMP 2) in a non-inverting configuration and with a gain of 45 ($G2 = 1 + \frac{R10}{R9} = 1 + \frac{68k}{1.5k} = 45$).

This way, both the A1 and A2 signals are amplified to the appropriate voltage level so that the microcontroller can now read them and detect the pulses. However, signal A1 is more amplified than signal A2. Thus, signal A1 was used to measure the heart rate in zebrafish, and signal A2 was used when testing on humans.

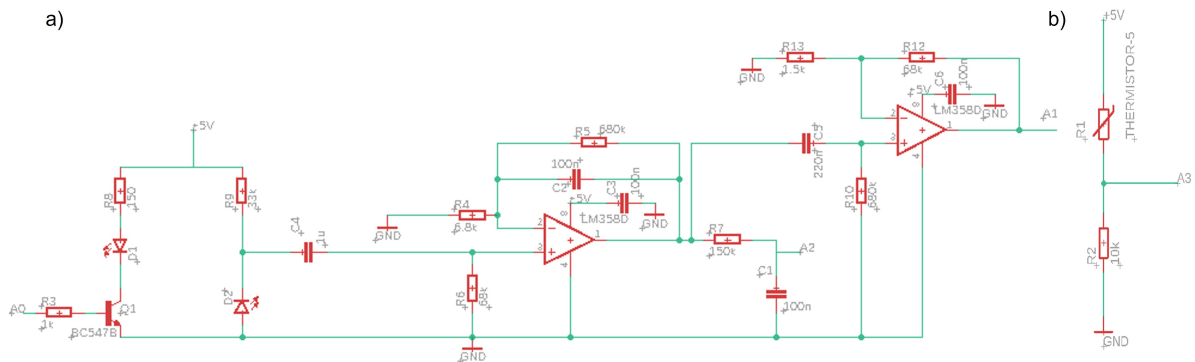


Figure 5.7: Signal conditioning circuit a) Heartbeat conditioning circuit. b) Thermistor conditioning circuit.

5.2.2 Water temperature conditioning circuit

The sensor chosen in this project to detect the water temperature was an NTC thermistor (10 kΩ, *BETATHERM*). As illustrated in Figure 5.7 b), the thermistor and a resistor (10 kΩ) were positioned in a voltage divider configuration to obtain a suitable signal for the microcontroller. The value of the resistor should be roughly equal to the resistance of the thermistor used, which is why it was used a resistor of 10 kΩ. Then, the signal (A3) produced by the variation of the thermistor resistance is read by the microcontroller.

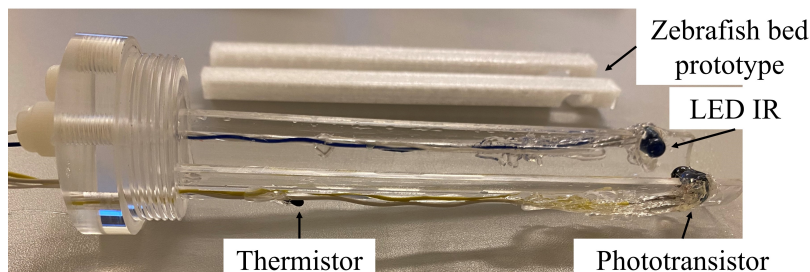


Figure 5.8: Image of the final version of the sensors positioning in the bed and waterproofed.

As the heartbeat and water temperature sensors are placed underwater, it was needed to waterproof them. The thermistor chosen was already coated with *Black Stycast 2850ft*

epoxy, so it was already waterproof. The waterproofing of the heartbeat sensors was made using thermo-retractable sleeves and hot glue (Figure 5.8).

5.2.3 Firmware

This study uses an Arduino Uno R3, due to its simplicity, to read the signals produced by the sensors and respective conditioning circuits for posteriorly processing. Therefore, the Arduino Uno function is to receive the data from the signal conditioning circuits, convert it into a digital signal and, after, perform a specific function on the device. To program the microcontroller it was used the Arduino IDE.

First, the heartbeat and water temperature detection system's output and input signals were connected to four analog ports (A0, A1, A2, and A3). The Arduino board has a 10-bit Analog-to-Digital Converter (ADC) that can convert the input voltage of the analog pins into integer values between 0 and 1023. This ADC is used for the output signals A1, A2 and A3. Subsequently, the pins are configured as an input (A0) and as an output (A1, A2, and A3), and a timer is initialised. The timer generates a periodic interrupt that calls an Interrupt Service Routine (ISR).

Posteriorly, the thermistor resistance value is converted to a temperature value in Celsius degrees. However, the Arduino UNO cannot measure resistance directly, only voltage. Thus, the microcontroller measures the voltage at a point between the thermistor and a known resistor (10 k Ω), which are in a voltage divider configuration. So, first, the analog reading on the pin A3 is converted to Volt ($V_o = 5 \times \frac{(float)analogRead(A3)}{1023}$). Then, it is calculated the resistance of the thermistor correspondent to the voltage based on the voltage divider formula ($R_{Thermistor} = R1 \times \frac{V_{in}-V_o}{V_o} = 10k \times \frac{5-V_o}{V_o}$). Finally, the Steinhart-Hart equation is used to convert the resistance of the thermistor to a temperature reading. The equation is 5.1 where T is the temperature (in Kelvin), R is the thermistor resistance at temperature T (in Ohm), and C1, C2, and C3 are the Steinhart-Hart coefficients, varying depending on the thermistor type and model. In this case, it were used the following values $C1 = 1.01 \times 10^{-3}$, $C2 = 2.38 \times 10^{-4}$, $C3 = 2.02 \times 10^{-7}$. Therefore, to convert the temperature to Celsius degrees, it is only needed to subtract the temperature in Kelvin by 273.15.

$$\frac{1}{T} = C1 + C2 \times \ln(R) + C3 \times \ln(R)^3 \quad (5.1)$$

In the ISR , the values of the analog pins (A1 and A2) are acquired using the Arduino function `analogRead(pin)`. Next, the timestamp of the values is obtained using a counter that is incremented inside the ISR . Finally, the signal A1 or A2, temperature, and timestamp are sent via serial communication to a Python program for further processing and displaying.

5.2.4 Software and Graphical User Interface

The data (sensor measurements) sent via serial communication from the Arduino UNO is received and processed by a specialised software developed in this project. This software was developed in Python due to its simplicity and powerful resources, and it was used multithreading and multiprocessing programming. Furthermore, the video recording component

of the software used a real-time optimised Computer Vision library called OpenCV. Besides, a GUI was also built to exhibit all information recorded by the sensors and the webcam. The GUI was built with the help of the tool QT Creator and integrated into the main software (Python). Thus, the present subsection explains how the software and GUI are structured.

To simplify the comprehension, in Figure 5.9 is possible to observe a block diagram of how the Python script is organised. Summarily, there is the main process (P1) where the thread T1 is created, which updates the user interface. Here, two different threads are created to process the data coming from the sensors (T2) and another for processing the images from the webcam (T3). The processes P2 and P3 establish the serial communication with the Arduino UNO and with the camera, respectively. Finally, the thread T4 is created to convert the frames to a QT image represented in the GUI . In Figure 5.10, there is a detailed representation of what happens in the different processes and threads.

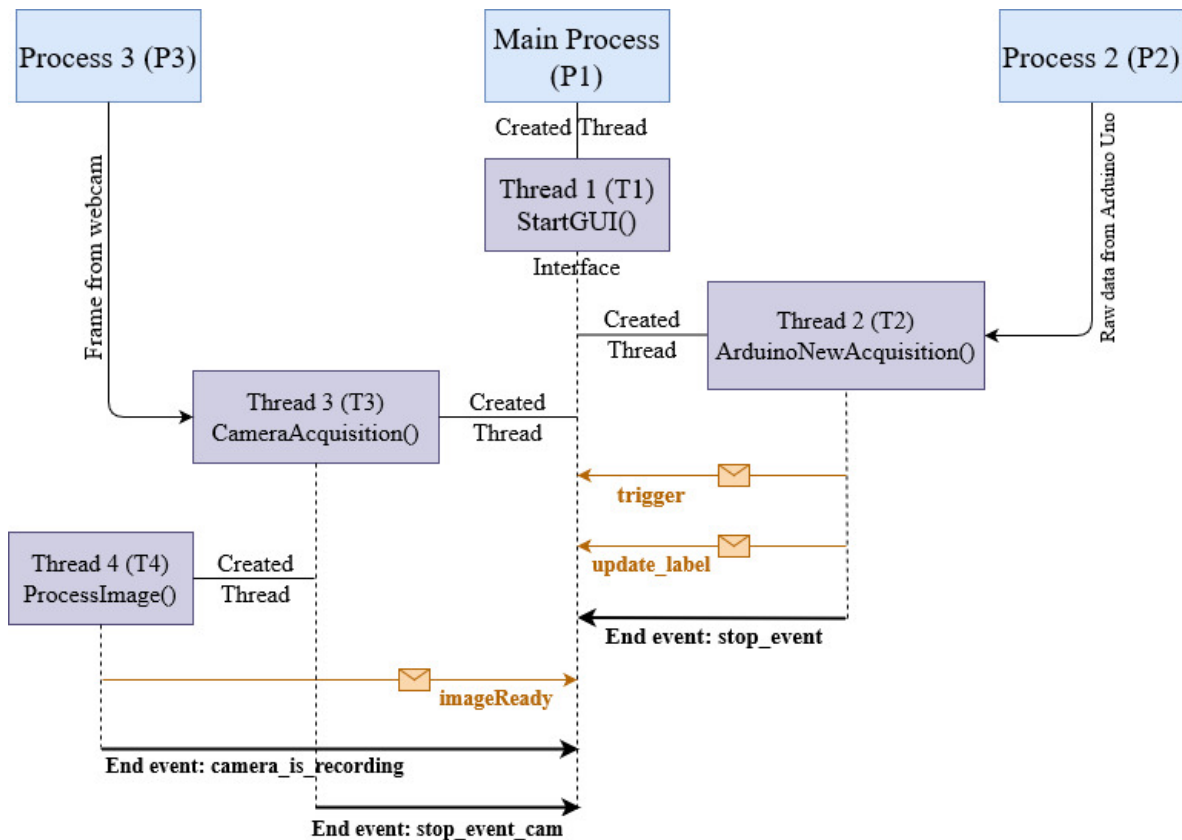


Figure 5.9: Block diagram of the Python script structure.

Notably, in T2, different tasks are performed. Firstly, an interprocess communication channel is opened (*Queue()*), enabling communication between P1 and P2. Then, the process P2 is booted, and a *while* cycle starts. In this cycle, the raw data read from the Arduino UNO is returned from P2 throughout the Queue, and posteriorly, this data is filtered. With this information, the heart rate and the mean temperature of the last ten seconds are calculated, and two signals (*trigger* and *update_label*) are sent to the thread T1 to update the interface with the updated values, posteriorly. The *trigger* is responsible for sending the filtered data to update the graph that displays the heartbeat. The *update_label* is responsible for sending

the heart rate and temperature values to update these values in the interface. The signals *trigger* and *update_label* are sent to the main every 25 samples and 250 samples, respectively.

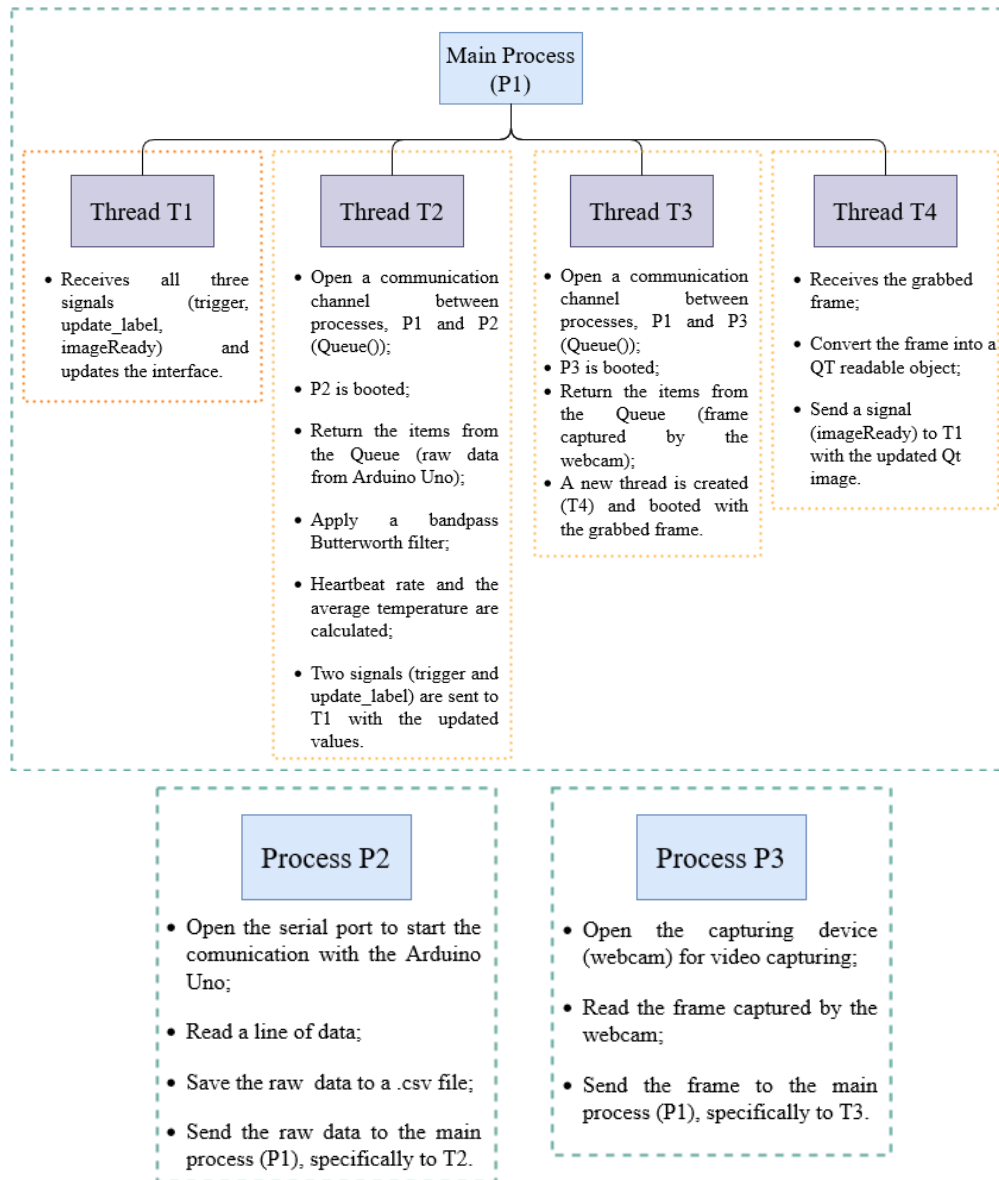


Figure 5.10: Detailed description of the role of each process and thread.

The raw data sent by the Arduino UNO was filtered using a bandpass Butterworth filter, implemented in Python, with cutoff frequencies of 0.2 Hz and 7 Hz. This way, both the DC component of the signal and higher noisy frequencies are eliminated. However, these frequencies suffered some adjustments depending on what was being studied. The heartbeat calculations used a Python function, *find_peaks*, that, as its name suggests, finds peaks (local maxima) inside a signal by a simple comparison of neighbouring values. This function takes several inputs that were adjusted to the signal under study to find the correct peaks. With the position of the peak information, it was viable to extract the time between two consecutive

peaks (Δt), and this way was possible to know the number of beats per minute ($bpm = \frac{60}{\Delta t}$).

In more detail, in P2, the serial port is opened, and then a line of data is read. This data is saved into a *.csv* file as soon as the camera starts recording. This timing is controlled by an event (*camera_is_recording*) that changes state when the camera sends the first frame. Finally, the last command in P2 is responsible for sending the raw data to the main process (P1) throughout the interprocess communication channel opened in T2.

In T3, there are also multiple tasks being realised. It also starts with opening an interprocess communication channel (*Queue()*), enabling communication between the P1 and P3 and following booting P3. P3 is responsible for reading the webcam's frames and sending them to the thread T3 via the interprocess communication channel. Then, if P3 reads a new frame, this frame is grabbed in T3, and a new thread T4 is created and booted. Finally, T4 receives the grabbed frame as an argument.

Lastly, to display the frames in the Qt interface, it was essential to convert them into a readable Qt object. So, this is done in T4 by changing the colour space BGR (blue, green, red) to RGB (red, green, blue), flipping horizontally the image, around the y-axis, and at last, using the function *QImage()*. When the conversion is finished, a signal (*imageReady*) is sent to T1 to update the Qt image displayed in the interface.

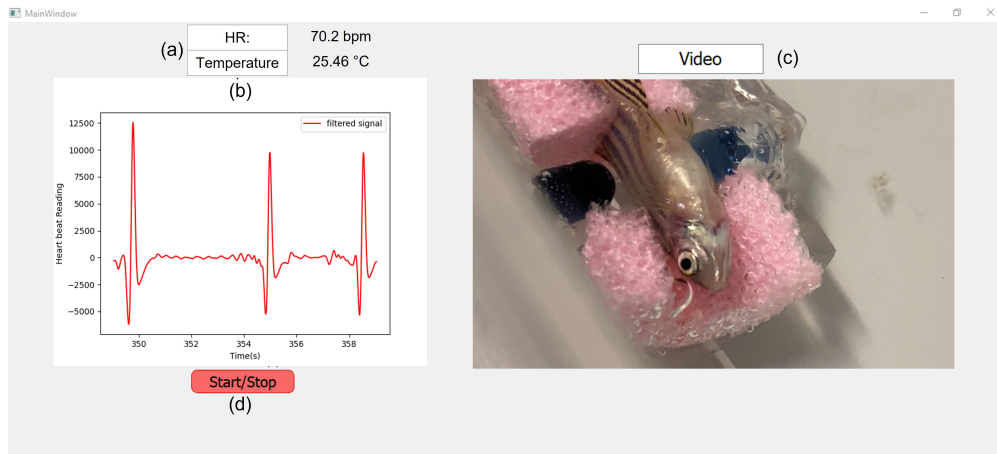


Figure 5.11: Graphical interface developed, during the signal acquisition.

As explained, several components in the GUI allow a better understanding of the fish status in real-time. Thus, in Figure 5.11 is possible to observe how the interface is organised. This figure shows the interface during the signals' acquisition. Therefore, the system starts when the user presses the button start/stop (d). Then, the data acquired by the sensors are displayed in the graph present in the interface (b). At the same time, the heartbeat frequency and temperature calculations are made and displayed in the interface (a). Also, the video captured by the camera is shown in real-time in the GUI (c).

The system start and stop process are controlled throughout the code with several events (*stop_event*, *stop_event_cam*, *camera_is_recording*) created in P1. These events change state according to the state of the button in the interface.

The monitoring software developed in the current dissertation and the code to later

analyse the data can be found in the following repository <https://github.com/ana-cata/DissertationAnaMagalhaes.git>.

5.2.5 Computer vision for heart rate detection

In order to confirm the results obtained by the sensors, an analysis based on computer vision was developed for heart rate detection. The software was developed in Python and using the OpenCV library. The basic principle of this video analysis software is that when zebrafish's heart beats, there is a change in the pixel's value in the heart region. Therefore, the software converts the frames to grayscale (pixel's value vary between 0 and 255) and allows the user to choose a Region of Interest (ROI) (Figure 5.12). Then, it calculates the pixels average value of that area for all frames of that video. Lastly, these values are saved into a file for posterior analysis. This way, when representing these values as a function of time, it is possible to verify the signal corresponding to the heart rate. Posteriorly, the function *find_peaks* was used to calculate the heart rate, similarly to what was done with the sensors' signals.



Figure 5.12: Interface of the computer vision software.

Chapter 6

Evaluation and validation of the acquisition environment

Several studies were carried out to validate some hypotheses relative to the behaviour of zebrafish under the anaesthesia effect (oxygen consumption, water temperature and pH evolution) and to verify if the developed monitoring system worked. Therefore, this chapter is divided into three sections. The first section explains how the stability of the dissolved oxygen and pH were evaluated, over time and in a closed environment, without water circulation. The second section exposes the evolution of the water temperature during the zebrafish experiments. Lastly, section three evidence the validation of the heartbeat detection system in human volunteers.

6.1 Dissolved oxygen and pH measurements

Before testing the zebrafish enclosure and the monitoring system for measuring heart rate and water temperature, it was necessary to ascertain whether the fish was stable for about 25 min without renewing water. Also, it was essential to understand if it was possible to realise a PET exam with a closed enclosure without water circulation. Therefore, it was decided to monitor pH and dissolved oxygen over time since these two parameters are checked more regularly in zebrafish tanks. Hence, a multi-parameter system (*Multi 3410*) was used with digital sensors, one for pH (*SenTix® 940*) and another for dissolved oxygen (*FDO® 925*). First, the zebrafish were anaesthetised and then transferred to a close recipient with a volume similar to the zebrafish chamber designed in this project to realise a PET exam, as shown in Figure 6.1. However, as the dissolved oxygen probe demands a water flow, it was needed to use a magnetic stirrer to ensure that the water crosses the sensor's membrane for accurate measurements. So, the setup needed to be adjusted for this measurement, as shown in Figure 6.1 a). To evaluate how the pH and dissolved oxygen vary over time, these values were registered every thirty seconds. Moreover, different zebrafish were used, some in a setup without agitation (Figure 6.1 b)), once the pH probe does not need it, and others in a configuration with water agitation. Finally, two control studies were also realised, without zebrafish, one with agitation and another without agitation.

The results of the dissolved oxygen consumption and pH evolution over time are shown in Figure 6.2, where the shaded region of the graphics corresponds to the respective probe errors. Analysing Figure 6.2 a), it is observed that the dissolved oxygen concentration decreases when the zebrafish is introduced in the recipient that contains the probes, which indicates that the zebrafish consumes some of the present oxygen. Relative to the pH graph (Figure 6.2 b)), it is possible to verify that the sensor takes some time to stabilise. However, after that period, it is observed that the pH follows the tendency of the control study. Thus, both graphs evidence that the zebrafish alters the environment concentration of dissolved oxygen and pH minimally. Nevertheless, dissolved oxygen and pH values remain within acceptable values throughout the experiments, between 6 – 8 mg/L and 6 – 8, respectively. Since the variations are so minimal it is possible to extrapolate that the zebrafish could be maintained stable for a few more minutes, corresponding to the necessary time to do a PET exam (around 30 minutes). In short, given the results obtained, it was possible to conclude that there is no need to increase the system's complexity to include water circulation on the zebrafish enclosure.

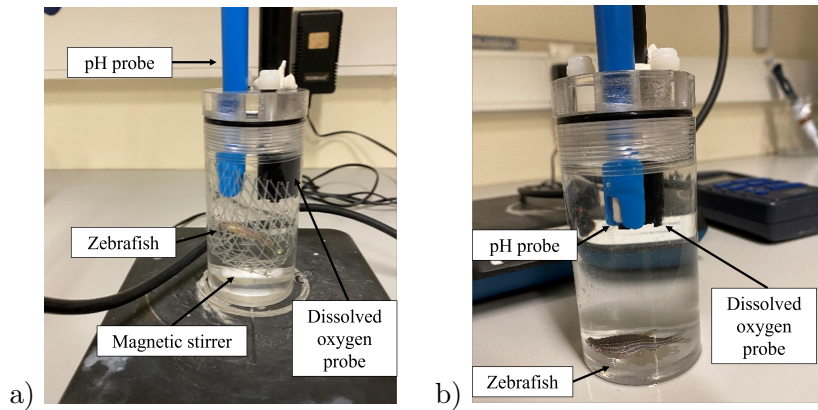


Figure 6.1: Setup to measure the dissolved oxygen and pH of the water a) with a magnetic stirrer, and b) without a magnetic stirrer.

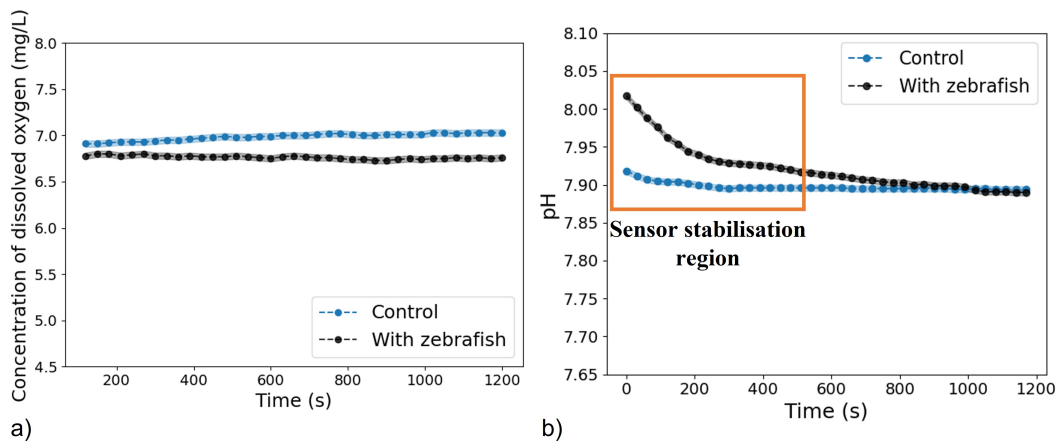


Figure 6.2: Variation of the a) concentration of dissolved oxygen and b) the pH over time with zebrafish and without (control).

6.2 Water temperature measurements

The water temperature was also evaluated using a thermistor during the zebrafish measurements trials since it is a parameter regularly checked in zebrafish tanks.

The water temperature evolution during a set of zebrafish heart rate measurements is observed in Figure 6.3. It is verified that the value remains around 24.5 °C and 25.5 °C, which is between 24 – 29 °C, the ideal range for zebrafish. There were moments during the trials when it was necessary to adjust the fish positioning. Therefore, it generated some movement in the water, leading to rapid changes in the thermistor response, as shown in Figure 6.3.

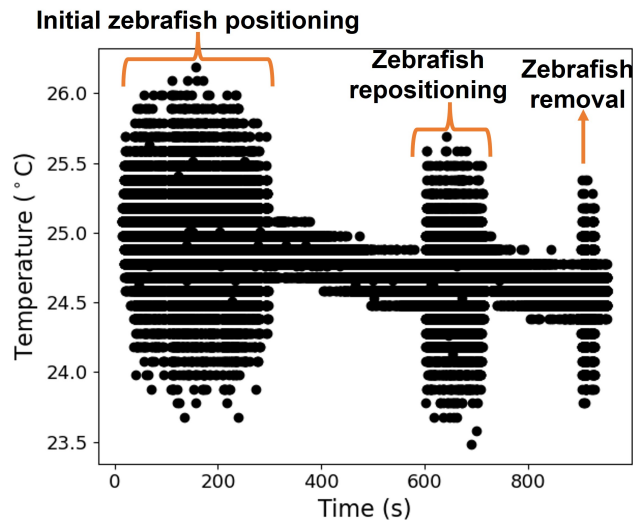


Figure 6.3: Water temperature evolution during a zebrafish trial.

6.3 Validation of the vital signs monitoring system

Afterwards, before testing the system in zebrafish, it was verified its functioning in humans. In this sense, a commercial heart rate meter (Oximeter *MD300C29*, *ChoiceMMed*) was used in order to compare its operation with the system developed during this work. Four volunteers were asked to put one finger on the commercial heart rate meter, and another finger from the other hand between the IR LED and the phototransistor. The volunteers remained in this position for about two minutes, and the pulse rate was registered from both heart rate meter and sensors every ten seconds. It was observed that there was no significant discrepancy between values. Besides, the same protocol was realised underwater, and it did not influence the sensor's measurement, as expected.

The results of the monitoring system's function are illustrated in Figure 6.4. Notably, Figure 6.4 only has the signals acquired from two volunteers because the other signals follow the same tendency as those represented. The slightly changes of the heart rate values over time observed in the graphs can be due to some agitation or stress of the volunteers caused by the measurement per se. Besides, the differences between the sensors and the commercial meter may be because it is more challenging to position the finger without moving it in the

system developed, and this movement can influence the sensor measurements. Despite some minor differences, the heart rate values calculated by the developed system are between the error range of the commercial heart rate meter, which indicates the correct functioning of the system developed.

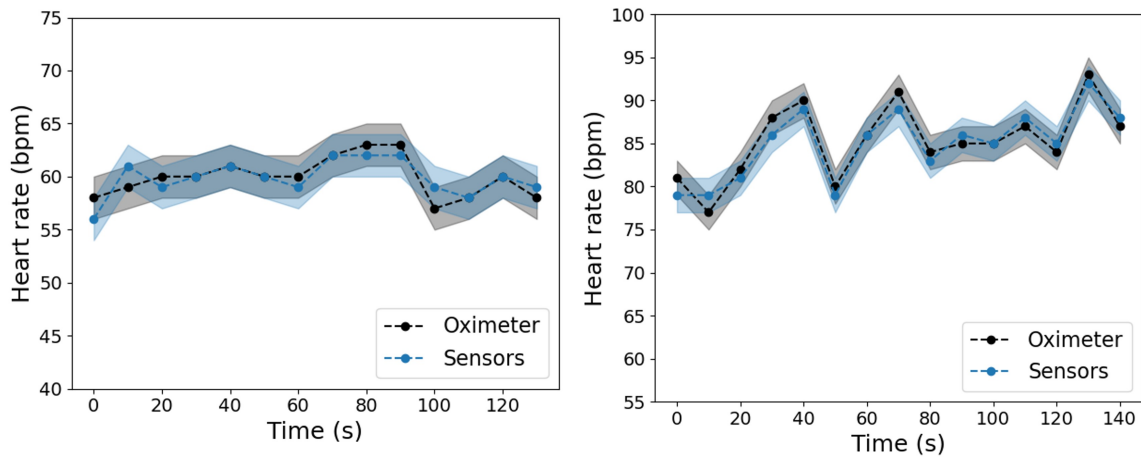


Figure 6.4: Graphics that compare the heart rate values obtained by the developed system's sensors and a commercial heart rate meter in two different volunteers.

Chapter 7

Zebrafish vital signs measurements

During the acquisition environment evaluation and the heartbeat detection system validation, discussed in the previous chapter, it was possible to assure that the pH and dissolved oxygen values remain stable over time and that the heartbeat detection system works properly.

Zebrafish vital sign measurements were performed in the Biology Department bioterium of the University of Aveiro. Two main trials (trial 1 and trial 2), each using several zebrafish, were done in the present work.

According to the defined protocol, the zebrafish were anaesthetised in an MS222 solution of 125 mg/L and then placed inside the container with the MS222 solution with a concentration of 100 mg/L. Then, the anaesthetised zebrafish were carefully positioned in the bed with the sensors aligned with the fish's heart for signal acquisition. The signals acquired were observed in real-time in the developed interface.

Initially, the system was tested on three adult zebrafish. In this first approach in real context, it was necessary to verify if the fish's size relatively to the bed was well adjusted, if the positioning of the zebrafish in the bed was easily done and if the developed hardware and software worked properly.

From this first experiment, only noise and some opercular movement were detected by the sensors. This happened because the developed circuit was assembled in a perfboard, and some connections were not well welded, and therefore, vulnerable to interference. To address this issue, it was necessary to design the system's circuit on a Printed Circuit Board (PCB) to reduce the noise and add another amplification stage to amplify the signal. Also, it was noticed that the opercular movement would be a significant obstacle to detect the heartbeat movement with the developed system. Thus, the positioning of the zebrafish on the bed became crucial and an aspect to study on trial 1. Besides, it was observed that the zebrafish's heart was visible.

In trial 1, the setup illustrated in Figure 7.1 was used (bed without sponge). In trial 1, different zebrafish positions in the bed were tested in order to find out the one that led to the best signals. Based on the results of these previous study, in trial 2, a different bed configuration was used, a sponge was used to help the immobilisation, as shown in Figure 5.4. Also, in this trial, the zebrafish was left in the same positions for more time to obtain a more significant amount of data. Besides, as the operator could easily see the zebrafish's

heartbeat, a camera was installed and used to record its movement in trials 1 and 2. Thus, it was possible to compare the values of the heart rate calculated by both systems, the sensors and the video.

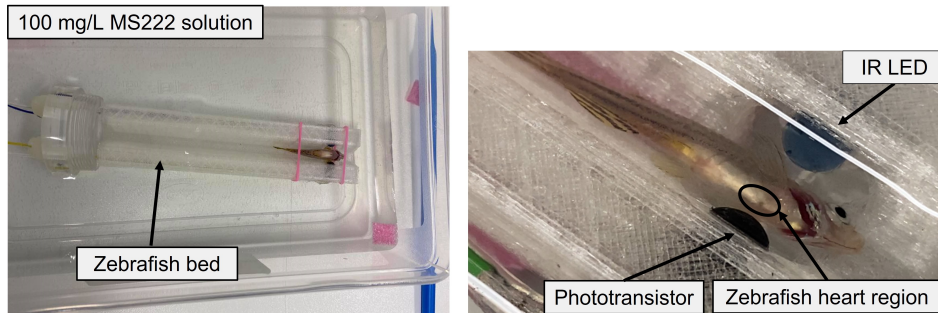


Figure 7.1: Setup used in trial 1.

a) Zebrafish heartbeat measurements - Trial 1

In this case, a set of five adult zebrafish was used to test the system. The first four zebrafish weighed between 380 mg and 440 mg and had already been used in another study, having been exposed to a heavy metal (lead), as presented in Table 7.1.

Table 7.1: Identification of the zebrafish used in trial 1.

	Zebrafish 1.1	Zebrafish 1.2	Zebrafish 1.3	Zebrafish 1.4	Zebrafish 1.5
Weight	435 mg	415 mg	440 mg	380 mg	740 mg
Gender	Male	Male	Female	Male	-
Lead exposition	Yes	Yes	Yes	Yes	No
Recovered anaesthesia	No	No	Yes	No	Yes
Time on anaesthesia (125 mg/L)	90 s	300 s	70 s	130 s	295 s

Additionally, in this experiment, it was noticed that the webcam installed in the system did not have enough quality to observe the zebrafish's heart. Hence, an additional camera, with better specifications, was added to record the zebrafish. Once the webcam was recording simultaneously as the sensors signal, it was used to synchronise the data acquired by the sensors with the video obtained from the camera.

A more detailed analysis of all signals acquired was done following the same procedure (Figure 7.2). First, the sensors signals were filtered using a Butterworth bandpass filter with 0.2 and 7.0 Hz cutoff frequencies. Then, the heart rate value is calculated based on the distance between two consecutive peaks. In addition, the signals were analysed in the frequency domain, using the Fast Fourier Transform (FFT). Then, a Gaussian curve or a sum of Gaussian curves was adjusted to the filtered data FFT. The mean of the adjusted Gaussian curve corresponds to the dominant frequency of the signal.

Moreover, the heart rate obtained by the sensors was compared with the value calculated using the developed computer vision algorithm for zebrafish heart rate detection. The

resulting signal from the camera was acquired at a sampling frequency of 30 Hz and passed by a Butterworth bandpass filter with 0.6 and 6.0 Hz cutoff frequencies. Then, the heart rate calculations were computed the same way for the sensors, with the *find_peaks* algorithm.

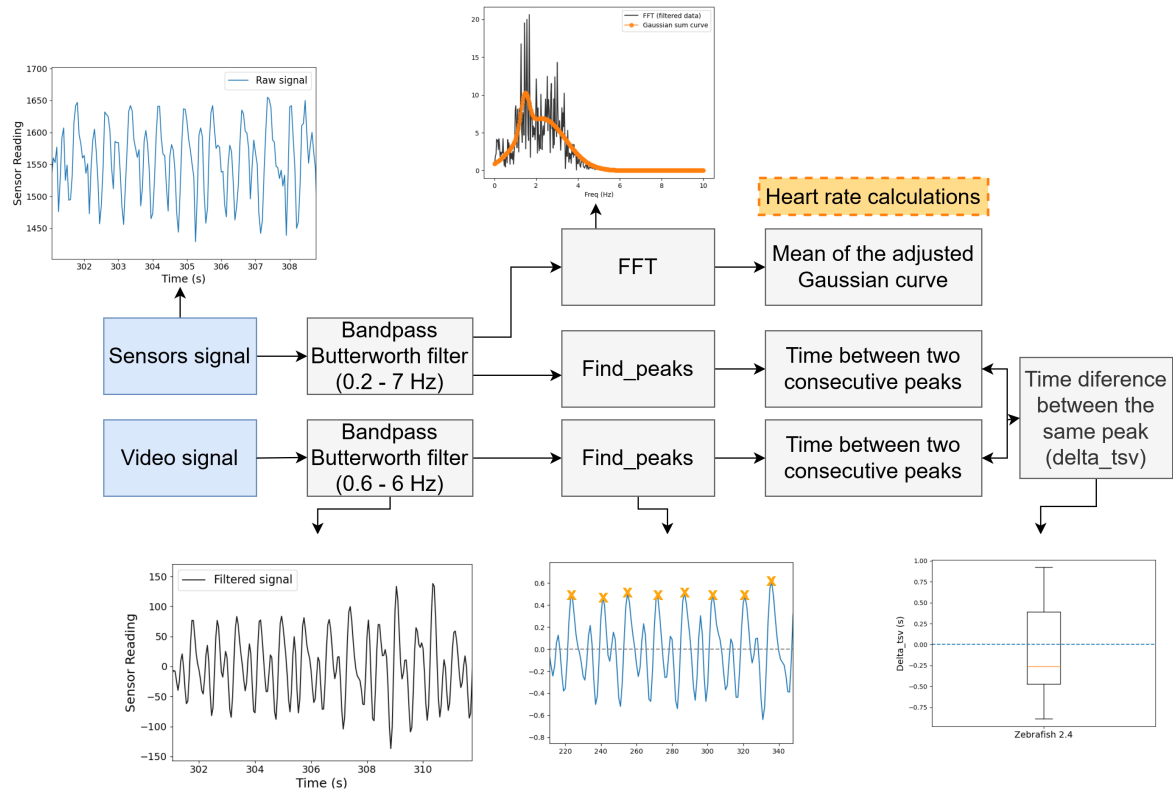


Figure 7.2: Block diagram of the analysis applied to the acquired signals, both by the sensors and the camera.

Moving on to a particular analysis of the acquired signals from each fish, in the case of zebrafish 1.1, it was only possible to acquire the signal of the operculum movement. As this was very intense, it overlapped with the heartbeat movement (Figure 7.3). Therefore, in the subsequent trial, zebrafish 1.2 was placed in the bed with the sensors placed a little below the operculum region, aligned with the fish’s belly. The signals obtained with zebrafish 1.2 are shown in Figure 7.4 a) and Figure 7.5 a). At the beginning of the acquisition, the zebrafish opercular movement was rare but present, as seen in Figure 7.4 a) (peaks with higher intensity). This signal also makes it possible to distinguish between the peaks that correspond to the zebrafish’s heartbeat (peaks with lower intensity) and the opercular movement. Towards the end of the acquisition, the opercular movement was nonexistent, so Figure 7.5 a) only shows the heartbeat pulse. Despite the zebrafish’s heartbeat being visible, the nonexistence of the opercular movement indicated that the zebrafish entered the overdose anaesthesia level (Table 2.3). Therefore, after placing the zebrafish in a tank filled with fresh water, it did not recover.

Regarding the zebrafish 1.3, it was possible to understand that it was incorrectly anaesthetised since it was constantly moving during the signal acquisition. Thus, the acquired signal shows a significant amount of noise, so the heartbeat pulse was impossible to identify.

For this reason, the signal is not represented once it is not relevant for the present work.

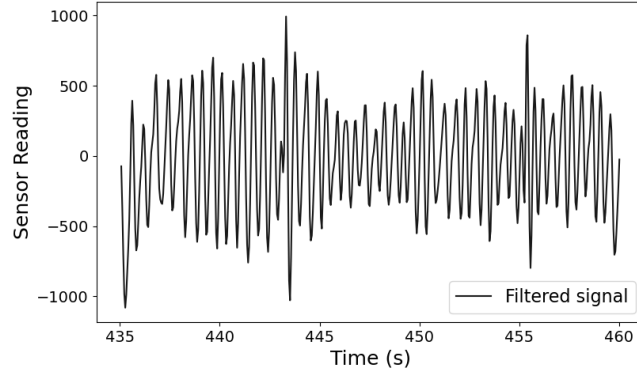


Figure 7.3: Signal acquired from zebrafish 1.1.

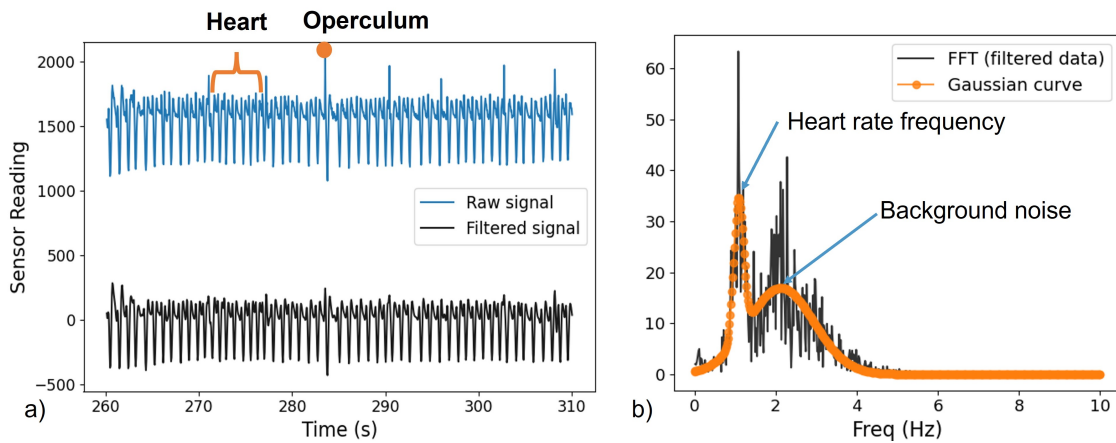


Figure 7.4: Signal acquired from zebrafish 1.2. a) At the beginning, signal with slow opercular movement (peaks with higher intensity) and with heartbeat pulses between the operculum peaks. b) FFT of the filtered signal represented in a) and respective Gaussian sum curve adjusted.

Passing to zebrafish 1.4, this one had a behaviour similar to zebrafish 1.2, a slow opercular movement initially and then absent towards the end, when only the heartbeat signal was present (Figure 7.5 b)). Like zebrafish 1.2, zebrafish 1.4 did not recover from anaesthesia.

Once zebrafish 1.2 and 1.4 did not recover from anaesthesia after the signal acquisition, it was necessary to understand why this was happening. Hence, it was decided to use a fifth zebrafish (1.5), but this time, an heavier zebrafish that was not exposed to lead was chosen. Figure 7.6 shows the signal acquired from this zebrafish. As the opercular movement was very intense, the signal only evidenced this movement. However, in the zoomed part of Figure 7.6, it is possible to observe that a small signal shows up when the opercular movement stops. This result indicates that it is possible to detect the heartbeat. However, it has some challenges regarding the opercular movement.

Analysing the graph of Figure 7.4 b), it is possible to observe that the curve adjusted

to the FFT is the sum of two Gaussian curves. The second one corresponds to background noise. Since this signal only has one element (heart), the mean value of the principal Gaussian curve adjusted coincides with the heartbeat frequency.

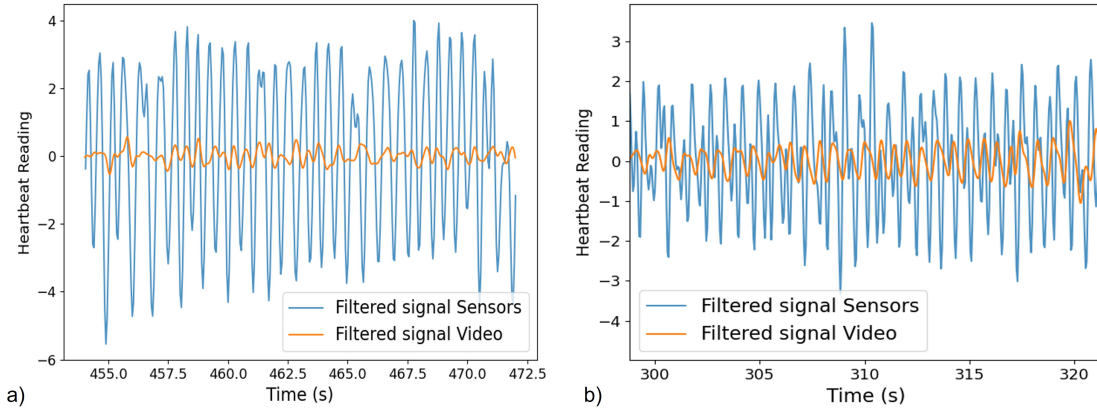


Figure 7.5: Signals acquired by the sensors (blue) and by the camera (orange) towards the end with only heart movement from a) zebrafish 1.2 and b) zebrafish 1.4.

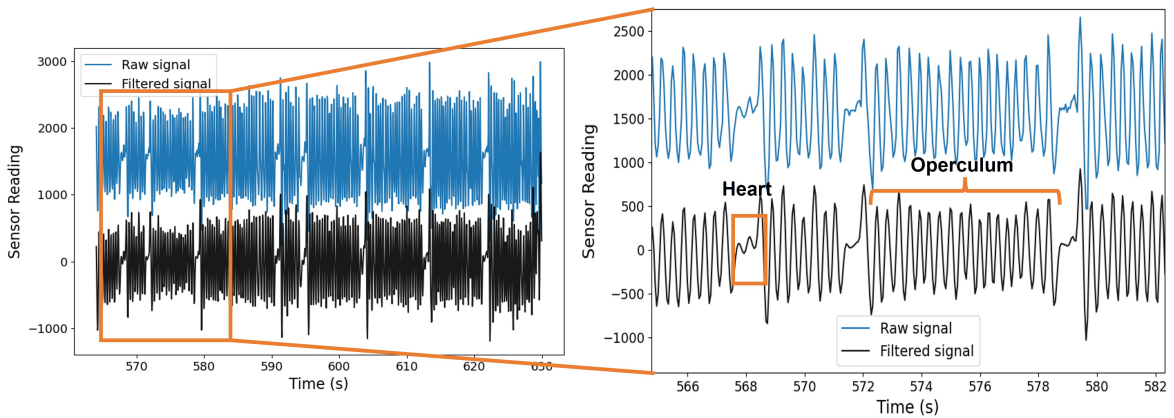


Figure 7.6: Signal acquired from zebrafish 1.5, correspondent to the opercular movement and respective zoom of the signal.

The video and FFT analysis were done to every zebrafish's signals, and the values obtained are referenced in Table 7.2. Thus, throughout the analysis of Table 7.2, it is possible to verify that the heart rate is similar between the *find_peaks* algorithm and the FFT. This happens because the frequency of the signals is well defined.

Now comparing precisely the heart rate values obtained by the video analysis and the sensors (Table 7.2), in the majority of the cases, the sensors heart rate value is situated within the error range of the video analysis. This indicates that the sensors correctly calculated the zebrafish heart rate. Unfortunately, the video of the zebrafish 1.2 has slight illumination changes, so it was impossible to calculate the heart rate for this fish using video analysis

software. This shows a limitation of the video analysis. Also, possible discrepancies can be due to some movement in the water which influences the sensors' measurement.

Table 7.2: Zebrafish heart and operculum rates calculated using three different approaches applying the algorithm *find_peaks* in the sensors and the video signals, and the mean value of a Gaussian curve adjusted to the FFT of the signal obtained by the sensors.

Signal	Signal observations	Sensors find_peaks (bpm)	Sensors FFT (bpm)	Video find_peaks (bpm)
Zebrafish 1.2 (Figure 7.4 a))	Operculum	10 ± 2	-	-
	Heart	65 ± 4	65 ± 12	-
Zebrafish 1.2 (Figure 7.5 a))	Operculum	Nonexistent	Nonexistent	Nonexistent
	Heart	115 ± 15	109 ± 25	114 ± 16
Zebrafish 1.4 (Figure 7.5 b))	Operculum	Nonexistent	Nonexistent	Nonexistent
	Heart	83 ± 12	88 ± 12	89 ± 13
Zebrafish 1.5 (Figure 7.6)	Operculum	166 ± 15	163 ± 25	160 ± 7
	Heart	-	-	104 ± 15

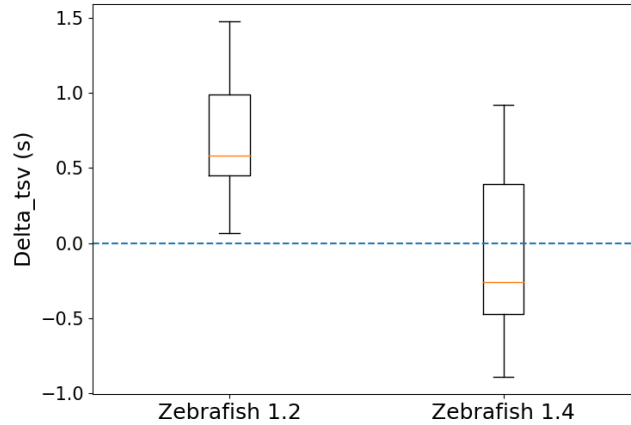


Figure 7.7: Box plot representing the dispersion of the time difference between the same sensors and video peaks of the zebrafish 1.2 and 1.4 signals.

Additionally, in Figures 7.5 a) and b), it is possible to confirm the similarities between the signals obtained by the sensors and the camera. Consequently, the box plot of Figure 7.7 demonstrates the peak dispersion of both approaches. In other words, these graphs have represented the time difference between the same peak in both signals (*delta_tsv*), which means that the closer the difference is to zero, the closer the sensor and video peaks are. In

both graphs there is a dashed line that represents the ideal scenario. In the box plot of the zebrafish 1.2 (Figure 7.7), it is possible to see that the box is situated above the zero's dashed line and that 50 % of the data is situated between 0.5 s and 1 s; this could happen because, in one of the methods, a peak was not identified, and therefore the error was propagated to the forward peaks' time. Relatively to the box plot of zebrafish 1.4 (Figure 7.7), the mean value of Δ_{tsv} is around -0.25 s, which is closer to zero. So, it is possible to affirm that both methods correctly measure the zebrafish heart rate.

Despite the promising results obtained in this trial, there were some aspects to improve. One aspect is the zebrafish immobilisation since their positioning in the bed was not optimal, consequently, the zebrafish quickly changed position due to slight water motion, affecting the acquired signal. An additional concern was the fact that some zebrafish did not recover once the anaesthesia protocol has already been tested in other zebrafish. Therefore, in the subsequent trial, these aspects were taken into account.

b) Zebrafish heartbeat measurements - Trial 2

In trial 2, the zebrafish bed was altered, a sponge was added, allowing a better immobilisation of the zebrafish. The sponge enables the zebrafish to be kept in the same position for more time and, consequently, obtaining more data. In addition, only adult zebrafish without lead exposition and with a weight bigger than 600 mg were used. In Table 7.3, all information relative to the zebrafish used in this trial is identified.

Table 7.3: Identification of the zebrafish used in the trial 2.

	Zebrafish 2.1	Zebrafish 2.2	Zebrafish 2.3	Zebrafish 2.4
Weight	600 - 800 mg			
Gender	Female	Female	Male	Female
Lead exposition	No			
Recovered anaesthesia	Yes			
Time on anaesthesia (125 mg/L)	125 s	147 s	230 s	167 s

Moreover, in trial 2, the sampling frequency was increased from 20 Hz (used in trial 1) to 100 Hz, which means that more data was obtained. Besides, the analysis of the signals acquired from the sensors and the camera was done the same way as in trial 1 (Figure 7.2).

Moving on to the presentation of the results obtained in this trial, in Figure 7.8, it is possible to observe the signal acquired from zebrafish 2.1, with both operculum and heart movement visible.

Relatively to zebrafish 2.2, the signals acquired are slightly different from zebrafish 2.1. In Figure 7.9 is possible to observe the presence of both heart and operculum movements. The negative peaks (orange) and positive peaks (black) correspond to, respectively, operculum and heart peaks.

The zebrafish 2.3 was not well anaesthetised, and, consequently, moved during the trial compromising the signal acquired.

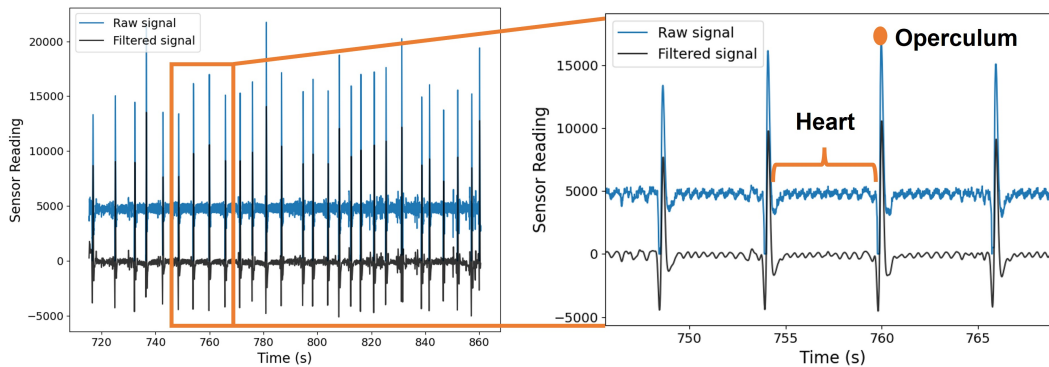


Figure 7.8: Signal acquired from zebrafish 2.1 and respective zoom of the signal.

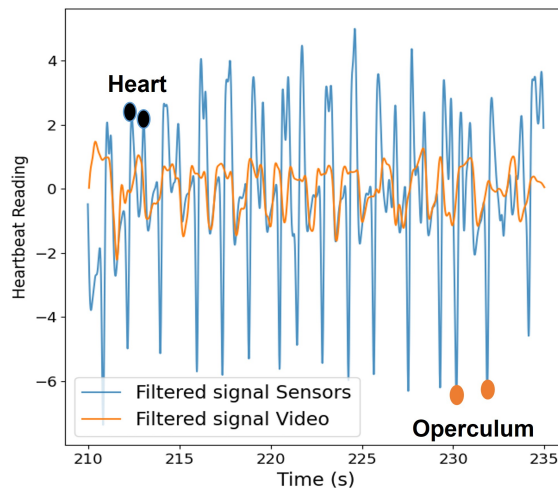


Figure 7.9: Signals acquired by the sensors (blue) and by the camera (orange) from zebrafish 2.2.

Regarding zebrafish 2.4, this had a similar behaviour as zebrafish 2.1. Thus, the signal acquired (Figure 7.10 a)) evidence both opercular and heart movements. Nevertheless, the opercular movement is more frequent, so it is more challenging to highlight the peaks corresponding to the heart movement. In Figure 7.10 b) it is possible to observe a region of the signal in which only the movement of the heart is present.

Once in the signals acquired from trial 2 it was possible to distinguish the heart movement from the opercular movement, the algorithm of *find_peaks* was adjusted to remove the peaks corresponding to the opercular movement when calculating the zebrafish heart rate.

Additionally, in trial 2, adjusting a Gaussian curve to the FFT of filtered data did not work as planned; since in the signals there were no well-defined frequencies. It is also possible to observe that the beating of the operculum and the heart are irregular, so the resulting FFT express a wide range of frequencies, making it impossible to distinguish a specific one.

Therefore for this trial, it was not performed FFT analysis.

In this way, the sensors and videos' signals were compared using the *find_peaks* algorithm, and Table 7.4 contains the heart rate values, which are similar to each other. The graphs of Figures 7.9 and 7.10 b) confirm the similarity between the two signals. The box plot of zebrafish 2.2 (Figure 7.11) shows that the majority of the time difference between the same peaks (*delta_tsv*) is less than zero, which means that it could exist a slight offset between the video signal and the sensors signal. However, this offset can be easily fixed. Relatively to the box plot of the zebrafish 2.4 (Figure 7.11), this has the mean of the peaks time difference near the zero's dashed line and 50 % of the time peaks are between -0.1 s and 0.1 s. Thus, despite some minor discrepancies, these results reinforce that the sensors correctly measured the zebrafish heart rate.

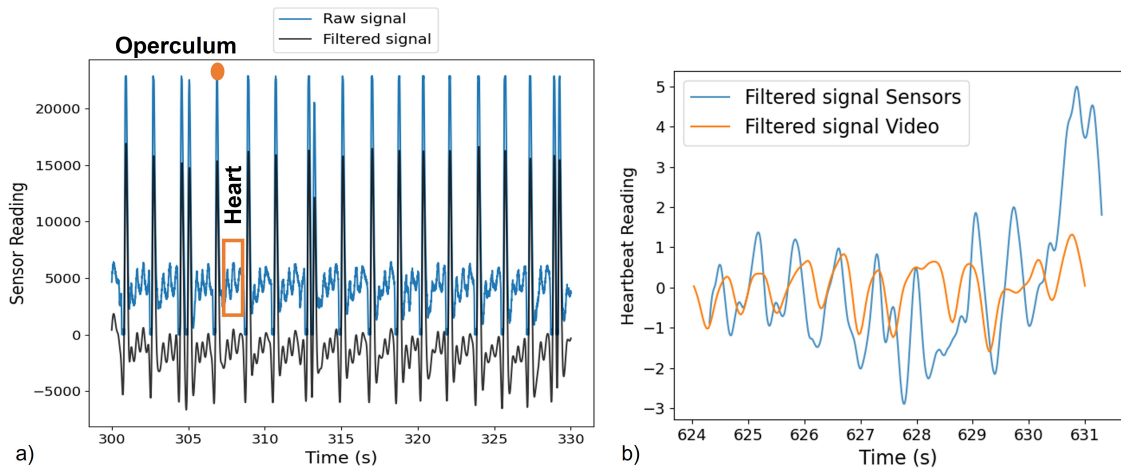


Figure 7.10: Signals acquired from zebrafish 2.4. a) General view of the signal. b) Particular region of the signal with only heart movement.

Table 7.4: Zebrafish heart and operculum rates calculated using two different approaches applying the algorithm *find_peaks* in the sensors signal, and applying the algorithm *find_peaks* in the video signal.

Signal	Signal observations	Sensors <i>find_peaks</i> (bpm)	Video <i>find_peaks</i> (bpm)
Zebrafish 2.1	Operculum	12 ± 3	12 ± 2
Figure 7.8	Heart	120 ± 10	127 ± 12
Zebrafish 2.2	Operculum	41 ± 11	49 ± 15
Figure 7.9	Heart	118 ± 4	117 ± 2
Zebrafish 2.4	Operculum	-	-
Figure 7.10 b)	Heart	88 ± 7	93 ± 2

Summarily, the developed system has some limitations regarding the zebrafish opercular

movement, but this can be overcome with correct anaesthetising. With this, the zebrafish has slow and regular opercular movement. This way, adaptations to the *find_peaks* algorithm (removal of operculum peaks) can be made in order to better identify the desired heart rate.

Lastly, the heart rate values obtained in trials 1 and 2 are acceptable compared to other literature studies shown in Table 2.4. Despite not following precisely the same pattern. For example, the heart rate of zebrafish 1.2 accelerates with time, against what is shown in Table 2.4. However, zebrafish 1.2 did not recover from anaesthesia and, at the end of signal acquisition, the fish could have accelerated its heart rate because it was under stress and entering a state of cardiac failure. In addition, the anaesthesia protocol followed in the present work, the time that the zebrafish were under anaesthesia effect, and the conditions under which the signals were acquired were different from those used in the literature. Therefore, the different protocols and environmental conditions could justify some minor discrepancies between the literature studies and the present dissertation.

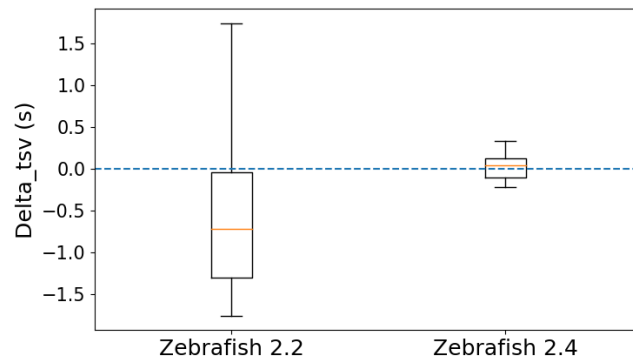


Figure 7.11: Box plot representing the dispersion of the time difference between the same sensors and video peaks of the zebrafish 2.2 and 2.4 signals.

Chapter 8

Conclusion

The increasing interest in zebrafish as a research model in the scientific community is due to characteristics such as its low cost, simplicity of maintenance on a large scale, inferior phylogenetic classification when compared with mammals, sequenced genome, ability to regenerate specific tissues, among others. This way, the zebrafish has enormous potential in research areas like genetic, regenerative and evolutive medicine. Still, they are excellent for models of human diseases such as cancer, cardiac diseases, cerebral diseases, obesity and diabetes. However, in the area of medical imaging, the zebrafish are underused mainly because its environment is aquatic. Therefore, it is necessary to develop additional tools and technologies that are resistant and capable of working in that environment. Another barrier is that the zebrafish are tiny and become hard to immobilise during the imaging exam. Additionally, it is difficult to anaesthetise them and to evaluate their well-fare by monitoring their vital signs accurately.

During this project, different components of the monitoring system and methodologies were tested and evaluated. First, the evolution of the water parameters, dissolved oxygen concentration and pH, were assessed. Since dissolved oxygen and pH do not vary significantly, it was concluded that a system with water circulation was not necessary to develop once the environmental conditions remained stable for zebrafish during the period of an easyPET imaging exam, between 5 to 30 min, depending on what is intended to study. Afterwards, the developed monitoring system was tested in humans, and its functioning was compared with a commercial heart rate meter. The results obtained were entirely satisfactory since the heart rate values calculated by the sensors of the developed system were similar to those shown by the commercial meter. In fact, the maximum difference between the heart rate obtained by the two methods was 3 bpm. In short, these acquisition environment studies allowed the verification of the system correct functioning, the right way to manipulate zebrafish and which conditions the zebrafish has to be in.

At this point, it was time to study the developed bed and monitoring system on zebrafish. Initially, the considerable influence of the opercular movement in the sensors was noticed. Also, it was observed that the zebrafish heart was visible. Therefore, for trial 1, the zebrafish positioning in the bed was studied, and a camera was coupled to the system. For trial 2, it resorted to other adult zebrafish, and for improving zebrafish immobilisation, it was used a sponge. The trial 2 signals remained stable over time and with both move-

ments, opercular and heart, confirming that the initial anaesthesia protocol worked properly for zebrafish, at least for those with more than 600 mg.

The signals obtained in trials 1 and 2 were reliable once they were in accordance with the signals obtained by the video analysis. The maximum difference noticed was 7 bpm, yet all sensors heart rate values were between the error of the computer vision method. The heart rate values obtained in both trials 1 and 2 were between 80 and 130 bpm, in accordance with the literature.

In summary, the system developed presents a promising path and the knowledge to its use in different imaging modalities and, consequently, its application in diverse studies combining zebrafish models and *in vivo* medical imaging.

8.1 Future Work

With the developed project and with its potential success, there is the need to evolve and even create a more robust zebrafish enclosure for the pre-clinic level.

This way, the future work will pass by improving and optimising the enclosure design to make the zebrafish manipulation and positioning inside the enclosure easier. For example, a rectangular enclosure with a window that opens to manipulate the zebrafish could be a possibility. To improve the system would also be essential to validate the developed system with a more significant zebrafish sample.

Another essential need will be the optimisation of the computer vision algorithm for zebrafish heartbeat detection. One strategy that could be implemented is the selection of two ROIs, one corresponding to the zebrafish heart and another corresponding to a region with few movements in the video, and then subtract the value of the two ROIs' pixels, which will decrease the influence of the illumination changes that occur during the trials. Alongside the algorithm, the need to improve the video quality and, therefore, the precision of the computer vision algorithm comes up. It would be a point in favour to incorporate a camera with better specifications, which could be an infrared camera.

Additionally, it would also be exciting to obtain a heart rate value in real-time using the computer vision algorithm. This way, combining the information obtained by the computer vision algorithm with the sensors' information, a better heart rate approximation could be achieved.

It is still proposed to elaborate a more rigorous protocol of the zebrafish preparation that can be adapted to different zebrafish sizes and different imaging modalities.

Finally, it is intended to incorporate the developed system in different medical imaging techniques and studies.

Bibliography

- [1] Gavin D. Merrifield, James Mullin, Lindsay Gallagher, et al. Rapid and recoverable in vivo magnetic resonance imaging of the adult zebrafish at 7T. *Magnetic Resonance Imaging*, 37:9–15, 2017.
- [2] Helene Volkoff. Fish as models for understanding the vertebrate endocrine regulation of feeding and weight. *Molecular and Cellular Endocrinology*, 497:1–13, 2019.
- [3] Zoe Swezy Browning. *Using Advanced Imaging to Study Fish*. PhD thesis, 2013.
- [4] Graham J. Lieschke and Peter D. Currie. Animal models of human disease: Zebrafish swim into view. *Nature Reviews Genetics*, 8(5):353–367, 2007.
- [5] W. Barbazuk, Ian Korf, Candy Kadavi, et al. The syntenic relationship of the zebrafish and human genomes. *Genome Research*, 10(9):1351–1358, 2000.
- [6] Ines J. Marques, Eleonora Lupi, and Nadia Mercader. Model systems for regeneration: Zebrafish. *The Company of Biologists Ltd*, 146(18):1–12, 2019.
- [7] Yali Zhao, Morgan Yun, Sean A. Nguyen, et al. In vivo surface electrocardiography for adult zebrafish. *Journal of Visualized Experiments*, (150):1–9, 2019.
- [8] Aswin L. Menke, Jan M. Spitsbergen, Andre P.M. Wolterbeek, et al. Normal anatomy and histology of the adult zebrafish. *Toxicologic Pathology*, 39(5):759–775, 2011.
- [9] P. Panula, Y. C. Chen, M. Priyadarshini, et al. The comparative neuroanatomy and neurochemistry of zebrafish CNS systems of relevance to human neuropsychiatric diseases. *Neurobiology of Disease*, 40(1):46–57, 2010.
- [10] Allan V. Kalueff, Adam Stewart, Robert Gerlai, and Palmer Court. Zebrafish as an emerging model for studying complex brain disorders. *Trends Pharmacol Sci.*, 35(2):63–75, 2015.
- [11] Priya Outtandy, Claire Russell, Robert Kleta, et al. Zebrafish as a model for kidney function and disease. *Pediatric Nephrology*, 34(5):751–762, 2019.
- [12] Robert J. Major and Kenneth D. Poss. Zebrafish heart regeneration as a model for cardiac tissue repair. *Drug Discovery Today: Disease Models*, 4(4):219–225, 2007.
- [13] Fiorency Santoso, Ali Farhan, Agnes L. Castillo, et al. An overview of methods for cardiac rhythm detection in zebrafish. *Biomedicines*, 8(9), 2020.
- [14] Louis W. Wang, Inken G. Huttner, Celine F. Santiago, et al. Standardized echocardiographic assessment of cardiac function in normal adult zebrafish and heart disease models. *DMM Disease Models and Mechanisms*, 10(1):63–76, jan 2017.
- [15] Richard Haindl, Abigail J. Deloria, Caterina Sturtzel, et al. Functional optical coherence tomography and photoacoustic microscopy imaging for zebrafish larvae. *Biomedical Optics Express*, 11(4):2137, 2020.
- [16] Avdesh Avdesh, Mengqi Chen, Mathew T. Martin-Iverson, et al. Regular care and maintenance of a Zebrafish (*Danio rerio*) laboratory: An introduction. *Journal of Visualized Experiments*, (169):1–8, 2012.
- [17] Hugh S. Hammer. Water Quality For Zebrafish Culture. In *The Zebrafish in Biomedical Research*, pages 321–335. 2020.
- [18] Jianfeng Feng, Ying Guo, Yongfei Gao, et al. Effects of Hypoxia on the Physiology of Zebrafish (*Danio rerio*): Initial Responses, Acclimation and Recovery. *Bulletin of Environmental Contamination and Toxicology*, 96(1):43–48, 2015.

- [19] Kerstin Howe, Matthew D. Clark, Carlos F. Torroja, et al. The zebrafish reference genome sequence and its relationship to the human genome. *Nature*, 496(7446):498–503, 2013.
- [20] G. Kari, U. Rodeck, and A. P. Dicker. Zebrafish: An emerging model system for human disease and drug discovery. *Clinical Pharmacology and Therapeutics*, 82(1):70–80, 2007.
- [21] Sandro Sieber, Philip Grossen, Jeroen Bussmann, , et al. Zebrafish as a preclinical in vivo screening model for nanomedicines. *Advanced Drug Delivery Reviews*, pages 1–17, 2019.
- [22] Harma Feitsma and Edwin Cuppen. Zebrafish as a cancer model system. *Molecular Cancer Research*, 1:229–231, 2002.
- [23] Anne Dorsemans, Christian Lefebvre d’hellencourt, Imade Ait-Arsa, et al. Acute and chronic models of hyperglycemia in zebrafish: A method to assess the impact of hyperglycemia on neurogenesis and the biodistribution of radiolabeled molecules. *Journal of Visualized Experiments*, (124):1–9, 2017.
- [24] Darya A. Meshalkina, Elana V. Kysil, Jason E. Warnick, et al. Adult zebrafish in CNS disease modeling: A tank that’s half-full, not half-empty, and still filling. *Lab Animal*, 46(10):378–387, 2017.
- [25] Lei Sun, Ching Ling Lien, Xiaochen Xu, et al. In Vivo Cardiac Imaging of Adult Zebrafish Using High Frequency Ultrasound (45-75 MHz). *Ultrasound in Medicine and Biology*, 34(1):31–39, 2008.
- [26] Monte Matthews and Zoltán M. Varga. Anesthesia and euthanasia in zebrafish. *ILAR Journal*, 53(2):192–204, 2012.
- [27] Chereen Collymore, Angela Tolwani, Christine Lieggi, et al. Efficacy and safety of 5 anesthetics in adult zebrafish (*Danio rerio*). *Journal of the American Association for Laboratory Animal Science*, 53(2):198–203, 2014.
- [28] Ana Pereira, Fernando Marins, Bruno Rodrigues, et al. Improving quality of medical service with mobile health software. *Procedia Computer Science*, 63(Icth):292–299, 2015.
- [29] Seyed Ehsan Mousavi and Jawahar G. Patil. Light-cardiogram, a simple technique for heart rate determination in adult zebrafish, *Danio rerio*. *Comparative Biochemistry and Physiology -Part A : Molecular and Integrative Physiology*, 246:1–13, 2020.
- [30] Wade Koba, Linda A. Jelicks, et al. MicroPET/SPECT/CT imaging of small animal models of disease. *The American Journal of Pathology*, 182(2):319–324, 2013.
- [31] Sean Kitson, Vincenzo Cuccurullo, Andrea Ciarmiello, et al. Clinical Applications of Positron Emission Tomography (PET) Imaging in Medicine: Oncology, Brain Diseases and Cardiology. *Current Radiopharmaceuticalse*, 2(4):224–253, 2009.
- [32] Kerstin Heurling, Antoine Leuzy, My Jonasson, et al. Quantitative positron emission tomography in brain research. *Brain Research*, 1670:220–234, 2017.
- [33] Jerrold Bushberg, Anthony Seibert, Edwin Leidholdt, et al. *The Essential Physics of Medical Imaging*. Number 2. 2002.
- [34] I. Mohammadi, I. F.C. Castro, P. M.M. Correia, et al. Minimization of parallax error in positron emission tomography using depth of interaction capable detectors: Methods and apparatus. *Biomedical Physics and Engineering Express*, 5(6), 2019.
- [35] Fábio António Lopes Carvalho. Procedimentos training em PET: Implementação no sistema easyPET. Master’s thesis, Universidade de Aveiro, 2017.
- [36] Ana Raquel Rocha Reis. *Aquisição , Processamento e Análise de Imagens de Medicina Nuclear*. PhD thesis, Universidade de Lisboa, 2012.
- [37] Valk P. E., Townsend D. L., Bailey abd D. W., and M. N. Maisey. *Positron Emission Tomography: Basic Sciencs*. Springer - Verlag London, 2005.
- [38] Kendra Bufkin and Matthew Leevy. Multimodal Imaging Trials with Zebrafish Specimens. *The Winthrop McNair Research Bulletin*, 1(3):1–5, 2015.
- [39] Emrys Jones, Fiona Henderson, Anthony Midey, et al. Comparison of lipid imaging in a zebrafish melanoma model by positron emission tomography (PET) and desorption electrospray ionization-mass spectrometry (DESI-MS). *Drug Metabolism and Pharmacokinetics*, 32(1):1, 2017.